EXPLORATORY STUDIES OF LIQUID BEHAVIOR IN RANDOMLY EXCITED TANKS: LONGITUDINAL EXCITATION

by

John F. Dalzell

Technical Report No. 1
Contract No. NAS8-20319
Control No. DCN 1-6-57-01042(1F)
SwRI Project No. 02-1869

Prepared for

National Aeronautics and Space Administration
George C. Marshall Space Flight Center
Huntsville, Alabama

May 1967

SOUTHWEST RESEARCH INSTITUTE
SAN ANTONIO   HOUSTON

SOUTHWEST RESEARCH INSTITUTE
8500 Culebra Road, San Antonio, Texas 78206

EXPLORATORY STUDIES OF LIQUID BEHAVIOR
IN RANDOMLY EXCITED TANKS:
LONGITUDINAL EXCITATION

by

John F. Dalzell

Technical Report No. 1
Contract No. NAS8-20319
Control No. DCN 1-6-57-01042(1F)
SwRI Project No. 02-1869

Prepared for

National Aeronautics and Space Administration
George C. Marshall Space Flight Center
Huntsville, Alabama

May 1967

APPROVED:

H. Norman Abramson, Director
Department of Mechanical Sciences

ABSTRACT

This report presents results obtained in an exploratory investigation of the behavior of fluid in a cylindrical tank under relatively low frequency random longitudinal excitation. It was found that large amplitude nonlinear free surface response is possible under some conditions of random excitation. Though quantitative data on free surface elevations were obtained only on the tank axis, the results strongly indicate that the large amplitude fluid response is of the 1/2 subharmonic type observed under harmonic excitation. Data on the probability structure of the nonlinear free surface response are also presented.

TABLE OF CONTENTS

NOMENCLATURE

a	Tank radius
B_d	Bond number
B_e	Effective filter bandwidth
d	Tank diameter
$\hat{F}(X_o)$	Estimated cumulative probability
$f(Y)$	Probability density
f	Frequency, cps
f_o	Center frequency (cps)
g	Acceleration of gravity
h	Depth of fluid in tank
$J_m(\ )$	Bessel function of first kind of order m
m, n	Indices
N	Tape speed ratio
$P(x), F(x)$	Cumulative probability
$q(A)$	Function of attenuator settings
r, ϕ, z	Cylindrical coordinate system
rms	Root mean square
$S_a(\Omega)$	Estimated acceleration spectral density
$S_x(f)$	Estimated spectral density at frequency f
$S_\eta(\Omega)$	Estimated fluid elevation spectral density
T	Sampling time
t	Time

iv

$X(t)$	Sample time history
$X(t, f_o, B_e)$	That portion of signal $X(t)$ which is passed by a narrow bandwidth filter with an effective bandwidth B_e and center frequency f_o
X	Standardized normal variate
Y	Standardized variate, doubly exponential distribution
γ	Euler's constant
$\Delta\Omega$	Nondimensional half power bandwidth
ϵ	Phase angle
η	Fluid elevation
$\bar{\eta}$	Estimated mean fluid elevation
ν	Surface tension
ξ_{mn}	Solutions of $\dfrac{d}{dr}\left[J_m(\xi_{mn}\frac{r}{a})\right]_{r=a} = 0$
ρ	Mass density
σ	Standard deviation
$\hat{\sigma}_a$	rms acceleration
$\hat{\sigma}_\eta$	rms fluid elevation
$\hat{\sigma}_x^2$	Variance of sample of $X(t)$
X_{mn}	mn^{th} free surface mode
Ω	Nondimensional frequency
Ω_{mn}	Nondimensional Eigenfrequencies, free surface
ω	Angular frequency
ω_{mn}	Eigenfrequencies, free surface

INTRODUCTION

Since fuel and oxydizers can account for as much as 90% of the lift-off mass of a launch vehicle, the dynamic forces exerted on the vehicle by the sloshing of these liquids can be relatively large. The central problem of interest insofar as the effect of propellant motions on rocket vehicles is concerned is that of stability and control. Generally speaking, sloshing of the liquid propellants will interact with both the control system dynamics and the vehicle structural dynamics, each of which also couple with the other. As the vehicle ascends, it is subject to random aerodynamic excitation in the form of noise, wind shears, transonic buffeting, etc. These perturb the flight path and excite both structural vibration and liquid sloshing, all of which must in turn be compensated for by the control system.

In reality, then, the excitation of the liquid propellants and their containing tanks must be random in nature. Due to the nature of the thrust control and the generally light construction of rocket vehicles, both lateral and longitudinal random excitation of the fuel tanks are experienced. Though the amount of literature available on the fuel sloshing problem is very great, Ref. 1, there seems to have been no attempt to explore experimentally the behavior of fluids in tanks under any sort of random excitation. It was the objective of the present program to fill this gap by experimentally exploring the effects of random excitation of cylindrical, partially filled, rigid tanks.

The scope and purpose of work in this project may be compactly summarized by quoting from the contract:

"Studies on liquid response to external excitations, so far, have been concentrated on deterministic processes in which the excitation of the tank is a definite function of time (primarily sinusoidal), and in which the response of the liquid is also deterministic.

This study shall deal with random processes, in which the excitation of the tank and the resulting fluid response can only be described in statistical terms. Since random excitations are prevailing under low-g conditions, this study has to be considered a first step to obtain some knowledge on this particular type of liquid response which shall be the basis of further exploratory research in this field.

The statistical nature of liquid response in random processes restricts this study primarily to experimental work. The specific objectives of this study shall include both lateral and longitudinal excitation of rigid cylindrical tanks. In the case of lateral excitation, the objective is to determine the validity of the linear assumption for force response under random excitation and to explore generally the problem of lateral liquid motion induced by random excitation. In the longitudinal excitation case the objective of this project is to explore the effects of random excitation on some of the nonlinear problems of sinusoidal excitation...."

The present report deals exclusively with the exploratory work carried out on random longitudinal low frequency excitation. The work carried out in the present program on random lateral excitation is dealt with in Reference 2.

Chapters 8 and 9 of Ref. 1 summarize the types of nonlinear problems encountered in experimental and analytical investigations of the fluid response to longitudinal sinusoidal excitation. These may be divided arbitrarily into four problem areas of varying size which will be briefly discussed under the headings:

1. Coupled Free-Surface Response in Longitudinally Excited Elastic Tanks

2. Bubble Dynamics in Longitudinally Excited Tanks

3. Spray Generation and Coupled Standing Wave Response

4. Low Frequency "Subharmonic" response

1. Coupled Free-Surface Response in Longitudinally Excited Partially Filled Elastic Tanks.

Of the large number of potential coupled fluid-elastic shell problems that exist, one that is the most interesting in the spirit of the present program has been called non-linear parametric coupling. Chapter 9 of Ref. 1, Refs. 3, 4 and 5, deal extensively with the subject. Under certain circumstances when a partially filled shell is excited sinusoidally near a "breathing" mode of vibration, a symmetric free fluid surface mode is excited at its modal frequency. The separation of elastic vibratory frequencies and symmetric fluid mode frequencies in this case may be two orders of magnitude. Since

the present program was limited to investigation of phenomena of rigid
tanks, an exploration of the effects of <u>random</u> rather than <u>sinusoidal</u> exci-
tation on this non-linear parametric coupling problem was not contemplated.
It should be remarked, however, that exploration of the influence of ran-
dom excitation in this case would be an interesting and possibly practical
area for future research.

2. Bubble Dynamics in Longitudinally Excited Tanks

This aspect of longitudinal excitation phenomena is well documented
in Chapter 8 of Ref. 1. Suffice to say here that at large, high frequency
vibrational input levels the free surface motion may become violent and
vapor bubbles are entrained in the liquid. Regardless of the origin of
the bubbles, they may become negatively buoyant if in a vibrating column
of liquid and migrate in unusual ways. The current status of the problem
is summarized in Ref. 6. Work on this problem was underway under
another contract at SwRI concurrent with the present program. In con-
junction with this separate program, preliminary experiments were
performed on bubble behavior in tanks subjected to random vibrational
inputs and the results are reported in Ref. 7.

3. Spray Generation and Coupled Standing Wave Response

At high longitudinal excitation frequencies the amplitude of free sur-
face motion is quite small. However, for certain combinations of(sinus-
oidal) excitation frequency and amplitude the small capillary waves formed
may disintegrate, form a dense spray, and under further restrictions
of conditions generate a much lower frequency standing wave. Again,
concurrent with the present program, this problem was under investigation
at SwRI in a separate effort. Exploratory experiments on the influence
of <u>random</u> excitation on spray generated fluid response were performed
in consultation with the present program and the results are reported in
Ref. 8.

4. Low Frequency "Subharmonic" Response

This problem area is in many respects the least complicated of
the four. For this reason, and because of the existence of the previously
mentioned programs in the preceding problem areas, it was selected
as the primary direct area of effort in the portion of the present program
devoted to longitudinal random excitation. Consequently, the investigation
described in this report is restricted to the "subharmonic" response
problem. In a subsequent section the applicable results from sinusoidal
excitation experiments will be outlined, and the work carried out and
results will be presented in a relatively standard sequence.

PRELIMINARY DISCUSSION, LIQUID RESPONSE
TO LOW FREQUENCY LONGITUDINAL EXCITATION

Analytical work on the response of the liquid free surface to low frequency longitudinal sinusoidal excitation is summarized in Chapter 8 of Ref. 1 and Ref. 9. The analytical work itself takes the form of a stability analysis for large amplitude free surface response, and the results are apparently sufficiently accurate to predict the (sinusoidal) frequency range where large amplitude motions should be expected. Qualitatively, under sinusoidal excitation, the liquid surface first experiences an instability in small motions and the resulting response is a nonlinear periodic motion. Since the stability boundary for the "1/2 subharmonic" occurs over a much wider frequency band (for a given level of excitation) than for the harmonic or the various super-harmonics, the nonlinear response is in the predominate form of a 1/2 subharmonic mode.

It should be noted that the terminology used herein differs from the usual in that the response under investigation is a nonlinear periodic motion which results only after an instability has occurred in originally small liquid motions. Since it occurs predominately at 1/2 the forcing frequency it has been loosely called 1/2 subharmonic response (Ref. 9), and this terminology will be maintained in this report. Similarly a response whose frequency is equal to that of the excitation will be called "harmonic" herein and a response whose frequency is a multiple of that of the excitation will be called "superharmonic".

Experimental confirmation in the sinusoidal excitation case is extensive, Ref. 1, 9. For sinusoidal excitation at a given frequency, and low amplitudes no large free surface motion occurs. What is first observed is a harmonic response. As excitation amplitude is increased toward the stability boundary the surface response can suddenly grow into a large amplitude "1/2 subharmonic" motion depending on the position of the stability boundary. Superharmonic response has also been found to occur under certain circumstances though with considerably smaller amplitudes than for the "1/2 subharmonic".

EXPERIMENTAL APPROACH

Since nonlinear random processes are not under very general control analytically, it is a problem of very large magnitude to extend available analytical results to the random excitation case. Consequently, in the present exploratory investigation, it was not feasible to design experiments to check any quantitative analysis, and the underlying philosophy of the investigation was to attempt to find out if the fluid free surface response under random excitation would behave qualitatively as expected from the previous sinusoidal excitation investigations.

In random excitation the describing parameters are necessarily slightly more complex than for sinusoidal excitation where a discrete frequency and an amplitude (of displacement or acceleration) suffice. For any random excitation at least 3 describing parameters and a specification of a probability distribution are required. In a practical sense the underlying probability distribution of experimentally produced random excitation very nearly has to be Gaussian (normal) and "stationary". The "normal" specification is because of the nature of available equipment, the fact that the literature on the normal distribution is the most extensive, and the fact that the result of a linear operation on a random Gaussian process is another random Gaussian process. The normal distribution is a one-parameter distribution which is completely described by the variance of the process (the mean squared deviation from the mean). In the present case it is more convenient to specify variance, or root-mean-square amplitude (abbreviated rms hereafter). The specification "stationary" means loosely that the statistical properties (variance, moments of distribution, etc.) do not change with time.

The rms amplitude of the excitation is not sufficient in itself to define the excitation for present purposes. The frequency band with which most of the energy (or mean square) is to be associated is also required and this must be defined by at least two parameters. Thus, experimentally, it would be necessary to deal with three parameters rather than two. In addition, in the random excitation case the excitation would contain energy over a continuous range of frequency.

The nature of practically realizable random excitation raised a basic question at the outset: "Does large amplitude fluid response exist at all under random excitation?" It was observed in Ref. 9 that the large amplitude response to sinusoidal excitation often took some time to develop, perhaps the proper conditions would not be present for a sufficient time under random excitation for anything much to happen. Supposing that large amplitude fluid motion is observed the next question might be: "Is large amplitude

5

free surface motion response to random excitation qualitatively similar to the "1/2 subharmonic" response observed in sinusoidal experiments and, regardless of whether it is or not, what might the probability structure of the response be?"

The first of the two questions outlined above required some crude experimental work even before proper excitation equipment was completed. It became possible early in the work to excite a 9" (22.8 cm) diameter tank randomly. No reasonably precise idea of the distribution of energy in the excitation could be obtained and no measurements were made, but visual observation confirmed that large amplitude free surface modes could be excited under at least a few experimentally realizable random excitations. No large anti-symmetric modes were observed, though it was clear that a great many modes could be excited at once.

These crude preliminary experiments in addition to advancing the investigation to the second of the questions posed in preceding paragraphs, made two additional points clear:

1. The excitation system should be capable of producing random excitation with sharply defined bands of energy since if excitation energy is present in equal levels, both at the frequency of the mode excited and at twice this frequency, there would be no way of distinguishing between a subharmonic response and a harmonic response. If the excitation energy band could be sharply attenuated between twice a modal frequency and the modal frequency, and a frequency analysis of the response made, a judgment might be made on whether the response was subharmonic or not according to the relative response energy levels. Response energy appearing at a frequency where excitation energy was very low would be indicative of subharmonic response.

2. In order to distinguish between subharmonic and harmonic response, some features of the free surface elevations would have to be measured and recorded as functions of time. The complexity of the free surface in the preliminary experiments would force some assumptions to be made on the nature of the response so that monitoring equipment could be selected.

Essentially it was assumed that the large amplitude free surface motion might be thought of as being composed of many superimposed natural modes. From a "pure" point of view this premise is undoubtedly

nonsense. From a practical point of view, adequate sampling and analysis of a time and space dependent random process requires effort of a much greater order than was within prospect. Consequently, the hypothesis that the spatial variation of the free surface could be described by the super-position of randomly excited natural modes in random spatial "phase" provided a conceptual link with available theory and previous experiment, and a "rational" means of choosing free surface elevation transducer systems for the experiments.

Since to a first approximation the surface elevation at the center of a cylindrical tank is composed of the contributions of only the axi-symmetric modes, it was decided to instrument the first test tank with a free surface elevation probe on the axis of symmetry, thus possibly only dealing with axi-symmetric mode response.

From the stability and control point of view, the anti-symmetric modal responses are of prime importance. The development was initiated in this program, of surface elevation measuring systems which would separate the lowest order anti-symmetric mode amplitudes and nodal orientations from all other possible modes. Several reasonable designs were achieved, Ref. 10, but were not reduced to practice within the present program.

Thus, the final experimental efforts in this phase of the project were oriented toward performing sufficient experiments to determine if the fluid elevation response to random longitudinal excitation on the axis of symmetry of a circular cylindrical tank was similar qualitatively to that which would be expected on the basis of sinusoidal excitation experiments, and to attempt an approximate determination of the distribution of this response.

EXPERIMENTAL APPARATUS

1. Tank and Transducers

The tank itself, Figure 1, was a 4-1/2 inch (11.4 cm) I.D., 1/4" wall, piece of plastic tubing bonded to an aluminum base plate which was suitable for attachment to the armature of a 1600-lb. Unholtz-Dickie electrodynamic shaker, Fig. 2. The variation of the I.D. of the tubing from perfectly circular was about $\pm 3/4\%$ of diameter. The selection of this particular size of tank was a compromise involving as large a size as possible consistent with shaker capacity. (This resulted in a somewhat smaller tank than can be accommodated for sinusoidal test purposes.)

For all tests reported herein, the tank was filled with distilled water (at about 70°F) to a depth of one tank diameter.

For reasons mentioned previously, a fluid elevation probe on the axis of symmetry was required. This transducer (which can be seen in Figure 1) consisted of a piece of No. 26 magnet wire (Niclad insulation) stretched along the tank axis and insulated from the tank base. This capacitance wire was connected in the internal bridge circuitry of a Tektronix Type Q transducer and strain gage unit with some minor modifications to result in an output proportional to changes in capacitance of the wire. With a Tektronix Type 133 power supply the wide open measuring system sensitivity was about 0.01 inches of surface elevation per volt output, deviations from linearity were $\pm 1/2\%$. An internal standard calibrating capacitor was installed corresponding to an 0.50 inch fluid elevation change. Repeated checks of this standard were carried out during the course of the experiments by varying the level of the water by draining and filling.

It was necessary to choose an "input" to the tank and the acceleration of the tank base was selected instead of displacement which had been the "input" measurement in previous studies. This choice was predicated as much by what was considered convenient for the relatively broad bands of frequencies and potentially large displacements contemplated, as by noting that acceleration of the tank is fundamentally the excitation involved in the analytical developments, Ref. 1, 9.

Since the accelerometer built into the armature of the shaker was of a type not intended for low frequency work, it was necessary to mount another accelerometer on the base plate of the tank. The only units readily

available which were sufficiently sensitive to meet the anticipated flow frequency—low g conditions were William Miller Type 402-C fluid damped, variable reluctance accelerometers. Unfortunately, the available amplification system for these units had too low an output level for magnetic tape recording, and it was necessary to use two of the variable reluctance units in a full bridge connection to enable operation with a Tektronix Type "Q" transducer and strain gage unit in a Type 133 power supply. This modified accelerometer system had good signal levels for magnetic tape recording, a wide open sensitivity of 0.004 g's/volt output, $\pm$ 1/2% linearity, and a flat frequency response to in excess of 50 cps. An electrical standard reference signal was installed and repeated checks of this standard were carried out during the experiments by statically calibrating the accelerometers on a tilt block.

2. Shaker System

The excitation signal (to be described) is basically a fluctuating voltage at the "input" to the shaker system. In the experiments it is most convenient to change the nature and/or the frequency content of this voltage. In practice, if the investigator wishes to have some notion during the experiment of the frequency distribution and level of acceleration, he is actually imposing on the specimen it is necessary to "qualize" the shaker system so that a given voltage input results in an essentially constant acceleration amplitude over the frequency range of interest. In the present case the 1600-lb electrodynamic shaker system in the Department of Mechanical Sciences Laboratory, was the best basic choice available, but since this system was not intended for low frequency work, its behavior in the frequency range of interest was unsatisfactory. A small direct coupled solid state power amplifier was built to clear up this problem, and having accomplished this it became possible to design and construct an equalizing filter and limiter amplifier to prevent occasional overdriving of the shaker and to flatten out the excitation system response over the range of frequency from about that of the lowest anti-symmetric fluid mode for the test tank to about 50 times this frequency. The final shaker system was open loop, that is: no feed back from the tank acceleration transducer was employed in the equalization. This was not necessary since freedom from serious amplitude distortion is attainable with filters. Phase distortion between excitation voltage and tank acceleration has no bearing when the accelerations are measured and recorded.

Because of the various mechanical and electrical safety limitations inherent in the equalized system, maximum peak to peak acceleration levels were limited to between 1/2 and 2 g's, depending on the frequency of excitation. Though higher limits might have been desirable, the system was judged adequate for the present exploratory work. Figure 3 is a photograph showing most of the equipment utilized in the experiments.

3. Excitation System

The central random excitation requirement is a source of Gaussian noise with uniform distribution of energy over the frequency range of interest. Since the frequencies involved in sloshing problems are below the audio range, a special low frequency noise source is convenient and in the present case an Elgenco Corp. Model 311A source provided a reliable Gaussian noise with frequency content from DC to 40 cps.

In the test program the rms acceleration level and frequency distribution were to be varied. This was done by interposing between the noise source and the equalized shaker system, various combinations of frequency band shaping filters (to be described) and a buffer amplifier with step input attenuator. The equipment used is shown in Figure 3. The buffer amplifier allowed adjustment of gain so that shaker acceleration amplitudes up to just under limiting could be achieved for each combination of shaping filters, the step attenuator was used to vary the excitation level.

During the experiments, three distinct methods of shaping noise were employed. The first, for "broad band" noise, was to filter the noise through two cascaded SKL variable cutoff active filters. One of these was set to control the low frequency cutoff, the other for the high frequency cutoff. The second method, for narrow band noise, involved the use of a Spectral Dynamics Corp. Tracking Filter with a (fixed) 2 cps bandwidth filter. With this equipment a 2 cycle wide band of noise at any desired center frequency could be picked out of the output of the noise source.

Since a 2 cycle bandwidth is actually "broad" relative to the separation of modal frequencies in the test tank, a method was sought to produce much narrower band random excitation signals. It was found that (with some care) it was possible to play back a signal previously recorded on one track of an Ampex FR 1800L Magnetic Tape Recorder while simultaneously recording data on other channels. This capability allowed the production of 1, 1/4 and 1/16 cycle band noise by time scale division of 2 cycle band random noise samples. By recording 2 cycle band noise at various tape speeds, excitation signals of various smaller bandwidths were produced upon playback at the lowest tape speed.

10

ANALYSIS EQUIPMENT

Analyses of random data commonly involve the estimation of the spectral distribution of "energy" (mean square deviation) of the process from a sample, the estimation of total mean square and, less commonly, estimation of the probability distribution function. The availability of the recorded samples of acceleration and free surface elevation on magnetic tape made analog analyses feasible. The lowest frequencies present in the data were such that playback of the tape 4 or more times faster than the recording speed resulted in apparent frequencies which fit comfortably within the capabilities of available analysis equipment. However, no loop recorder was available and thus any analog analyses attempted would have to be compatible with "shuttling" of tape back and forth, that is the rapid continuous frequency scanning methods in common use would have to be modified.

1. Spectral and Mean Square Estimates

Given a sample voltage time history $X(t)$ from a stationary random signal, the power spectral density function $S_x(f)$ for the signal may be estimated as in Eq. 1 (Ref. 11, for example),

$$\hat{S}_x(f) = \frac{1}{B_e T} \int_0^T X^2(t, f_o, B_e)\,dt \tag{1}$$

where:

$\hat{S}_x(f_o)$ = Estimated Spectral Density at Frequency f_o

$X(t, f_o, B_e)$ = That portion of the signal $X(t)$ which is passed by a narrow bandwidth filter with an effective bandwidth B_e cps and center frequency f_o cps.

T = Sampling Time

In words, the estimates are made by the following operations:

1. Frequency filtering of the signal by a narrow bandpass filter having an effective bandwidth of B_e cps and a center frequency of f_o cps.

2. Squaring of the instantaneous value of the filtered signal.

3. Averaging of the squared instantaneous value over the sampling time T .

4. Division of this mean square by B_e .

In the present case equipment was available to approximate the integral of the square by both RC filtering of the rectified, filtered signal, and by performing the square and an integration. However, nonlinear response, and thus non-Gaussian, signals were expected and the true mean square measurement was to be preferred.

An annotated functional diagram of the spectrum analysis system used is shown in Figure 4 and the physical setup in Figure 5. Referring to Figure 4, the first operation is a compression of time scale. The narrow band filtering was carried out by the same tracking filter used to generate some of the excitation signals. The center frequencies were set manually. The filtered signal was then attenuated as required to suit the square-law output of a true rms voltmeter. The output of the square law device was then frequency modulated and the number of cycles in this FM signal were counted over a controlled time interval. As noted in Figure 4, this count is proportional to spectral density. In order to calibrate this count the random signal was replaced by a known sinusoidal voltage and the system operated as for the actual spectrum analysis.

In operation, tape play back speed, filter bandwidth, and sampling time were selected, set up and recorded, step calibration signals on the tape before and after the sample were measured and the system constant for converting counter display to (volts)^2 was established. The operator started tape playback, selected a center frequency (f), and Ballantine attenuator (A) to yield a reasonable counter display, started the count of the sample, recorded the total count during the sampling time, and then adjusted the center frequency to the next value, and so on. When it was judged that sufficient point coverage of the frequency range had been achieved the operator moved on to another sample on the tape. Ultimately, a number representing the physical calibration of the data on the tape was added to the recorded data, all numbers key punched and in the CDC 160A digital computer operated by the SwRI Computations Laboratory, the analysis was completed by a) applying calibration constants compensated for attenuator settings to the counter outputs to convert to (engineering units)^2, b) this result was divided by bandwidth, B_e compensated for tape playback speed to result in dimensional spectral density, c) these spectral densities and the associated frequencies were non-dimensionalized, d) tabulated and e) rough plotted.

The variance of the sample, $\hat{\sigma}^2$, was estimated with the same equipment by by-passing the tracking filter, Figure 4. In this case the counter output is proportional to $\hat{\sigma}_x^2$ where:

$$\hat{\sigma}_x^2 = \frac{1}{T} \int_0^T X^2(t)\,dt \qquad (2)$$

Much the same procedure in calibrating the system for spectral density estimation was followed for variance estimation.

The selection of bandwidths, sampling times, tape playback speeds, etc., for the analysis of each taped data sample was made from statistical considerations and these will be discussed in a subsequent section.

2. Probability Distribution Estimates

Because an analog system for cumulative probability estimates $P(X)$ is easier to realize than one for probability density estimates, $\left(\frac{d}{dX}P(X)\right)$, this approach was chosen. If δt_i is the time spent by $X(t)$ above the level X_o during the ith excursion above X_o , the cumulative probability may be written (Ref. 11):

$$P\left(X(t) > X_o\right) = \lim_{T \to \infty} \left[\frac{\sum_i \delta t_i}{T} \right] \qquad (3)$$

and thus an estimate (Ref. 11) for the cumulative probability from a record of $X(t)$, T seconds long is:

$$\hat{F}(X_o) = \hat{P}\left(X(t) > X_o\right) = \frac{1}{T} \sum_i \delta t_i \qquad (4)$$

The method by which this estimate was realized is outlined in Figure 6. The sample signal from the magnetic tape was compared with a manually adjusted voltage reference (E_o) in a voltage comparator. The output of the voltage comparator actuated a gating amplifier which turned on and off a high frequency sinusoidal signal according to whether the sample signal was above or below the reference. This gated signal was counted over the time necessary for an integral power of ten cycles of the high frequency sinusoidal signal. Thus the need to perform any arithmetic on

13

the accumulated count was eliminated (apart from the decimal point) and the count was written down as the estimate, $\hat{F}(E_o)$. The process was repeated for as many reference levels as needed to define $\hat{F}(E_o)$ reasonably within the $\pm$ 3-1/2 σ range on normal probability paper.

Because the period of the gated high frequency signal is finite and because the voltage comparator and gate do not switch instantaneously, there are errors in the process. These were minimized by maintaining the frequency f_c (Figure 6) at 1000 cps, which was between 50 and 250 times the highest significant frequency in any of the records. The system was tested with sinusoidal inputs to establish the required magnitude of f_c , among other things, and it is felt from the good correlation and repeatability achieved with sine waves that the inherent errors in the estimate of $\sum_i \delta t_i / T$ will be far less than the sampling errors involved in relating $\hat{F}(E_o)$ with $P(E_o)$.

DIMENSIONAL CONSIDERATIONS

In the experiments, a free surface elevation and tank acceleration were measured as functions of time. In subsequent analyses of data, time as a parameter was replaced by frequency. While no representations are intended that the data to be presented can be extrapolated to any size tank, a non-dimensional presentation does facilitate comparisons with other experiments and with analytical results.

Therefore, all free surface elevations were divided by tank diameter, (d) and all accelerations by the acceleration of gravity (g). A convenient form for frequency nondimensionalization is

$$\Omega = \omega \sqrt{\frac{d}{g}} \tag{5}$$

where: ω = angular frequency.

These were carried through the spectral analyses to result in acceleration spectral density having dimensions of $(g)^2/\Delta\Omega$ and in free surface elevation spectra having dimensions $(diameter)^2/\Delta\Omega$.

From the point of view of correlation, Ref. 8, the "Bond number" is a nondimensional parameter of importance. In the present case for all experiments this number, based on diameter is:

$$B = \frac{\rho g d^2}{\nu} \approx 1750 \tag{6}$$

where ρ = mass density
ν = surface tension

For convenience, the first twenty eigenfrequencies of the free surface are tabulated in Table I in terms of the nondimensionalization of Eq. 5. The subscript $n = 0$ herein refers to the lowest frequency of the type of mode, m ; that is, the mode shapes are assumed of the form:

$$X_{mn} \propto \cos(m\phi + \epsilon) \, J_m(\xi_{mn}\frac{r}{a}) \tag{7}$$

15

TABLE I

The First Twenty Eigenfrequencies for a
Circular Cylindrical Tank (h/d = 1)

Frequency Order	m	n	Ω_{mn}	$2\Omega_{mn}$	Remarks:
1	1	0	1.92	3.84 ◄———	First Anti-Symmetric
2	2	0	2.47	4.94	
3	0	0	2.76	5.52 ◄———	First Axi-Symmetric
4	3	0	2.90	5.80	
5	4	0	3.26	6.52	
6	1	1	3.265	6.53	
7	5	0	3.58	7.16	
8	2	1	3.66	7.32	
9	0	1	3.75	7.50 ◄———	Second Axi-Symmetric
10	6	0	3.87	7.74	
11	3	1	4.00	8.00	
12	1	2	4.13	8.26	
13	7	0	4.14	8.28	
14	4	1	4.31	8.62	
15	8	0	4.39	8.78	
16	0	2	4.51	9.02 ◄———	Third Axi-Symmetric
17	5	1	4.58	9.16	
18	3	2	4.76	9.52	
19	1	3	4.84	9.68	
20	6	1	4.86	9.72	

where:

r = radial coordinate of a point on the free surface

ϕ = angular coordinate of a point on the free surface

m = 0, 1, 2 ....

n = an index, 0, 1, 2...

ϵ = a phase angle

$J_m(\ )$ = Bessel function of first kind of order m .

ξ_{mn} = solutions of: $\dfrac{d}{dr}\left[J_m(\xi_{mn}\dfrac{r}{a})\right]_{r=a} = 0$

a = tank radius

Eigenfrequencies are defined by:

$$\Omega^2_{mn} = \frac{\omega^2_{mn}}{g}\,d = 2\,\xi_{mn}\,\tan h\,(\xi_{mn}\,\frac{2h}{d})$$

$$\approx 2\,\xi_{mn}\,,\,\frac{h}{d} = 1 \tag{8}$$

where h = depth of fluid in tank, and the ξ_{mn} are tabulated in Ref. 1.

17

EXPERIMENTAL PROGRAM

1. Sinusoidal Excitation

In order to check that the present experiments would be related to previous experiments, a brief series of sinusoidal experiments were run to obtain a rough idea of the "subharmonic" response stability boundary for comparison with the experimentally determined general 1/2 subharmonic stability boundary obtained in Ref. 9. No experimental pains comparable to those in Ref. 9 were taken with these experiments. All that was done was to find 1) the rms acceleration level required to produce a barely resolvable harmonic response (0.0002 diameter amplitude) on the axis of symmetry and, 2) roughly establish a range of rms acceleration such that recognizable subharmonic response was observed at the high end, while large but still harmonic response was observed at the low end. The data was compared with the boundary presented in Ref. 9 after non-dimensionalizing both sets of data and converting displacements to rms accelerations in the case of the data from Ref. 9. The range from the present experiments, wherein the stability boundary should lie, bracketed the results from Ref. 9. The stability boundary from Ref. 9, converted to units compatible with those herein is shown in Figure 7. Also shown in this figure is a "threshold" of measurable harmonic response for the first axi-symmetric mode.

2. Random Excitation

In the random excitation program proper, 17 samples of acceleration and free surface elevation were obtained on magnetic tape. A summary of the program is contained in Table II. An attempt was made in the program to study both the influence of level of excitation and frequency distribution of acceleration.

The first type of excitation shown in the table, "ultra narrow band" was essentially a randomly modulated sine wave. It was centered on twice the frequency of the first symmetric mode. The excitation level was adjusted to the maximum possible without clipping or limiting the shaker (subsequently found to be .17 to .19 g's rms) and a sample taken. The excitation level for this excitation condition was then adjusted downward with a step attenuator. At approximately half the maximum rms level the 1/2 subharmonic response in the lowest axi-symmetric mode was much less prevalent visually. At 1/3 the maximum level of excitation signal, 1/2 subharmonic type response

18

TABLE II - Summary of Random Excitation Experiments

Nominal Type Excitation	Half Power Bandwidth ΔΩ	Center Frequency	Acceleration Levels, g's rms	Number of Samples
Ultra Narrow Band	0.04	Twice the frequency of first symmetric mode	.09 to .18	3
Very Narrow Band (1)	0.17	Twice the frequency of first symmetric mode	.08 to .17	3
Very Narrow Band (2)	0.68	Twice the frequency of first symmetric mode	.13 to .19	2
Narrow Band	1.36	Twice the frequency of first symmetric mode	.13 to .19	2
Narrow Band	1.36	Twice the frequency of second symmetric mode	.3	1
Narrow Band	1.36	Twice the frequency of third symmetric mode	.3	1
Narrow Band	1.36	At the first symmetric mode	.1	1
"Broad Band"	Various distributions of energy from first to beyond the 15th symmetric mode		.14 to .36	4

seemed for the most part not to be present. (Even at maximum excitation level there were periods of relatively little free surface response.) At this point in the experiment the assumption was made that the variation in rms excitation from maximum to half-maximum would substantially cover the transition range between predominant subharmonic response and predominant harmonic response for this type of excitation, and a sample was taken at this level and at 2/3 maximum level. These three levels of excitation were also set for the "very narrow band (1)" excitation. As the excitation bandwidth was increased for excitation centered at twice the first axisymmetric mode, less activity was noted for the half-maximum excitation level and this case was omitted for "very narrow band (2)" and "narrow band", Table II.

Data was recorded for three special cases of "narrow band" random excitation, Table II. The first was with excitation centered on twice the frequency of the second axi-symmetric mode, the second with excitation energy centered on twice the frequency of the third axi-symmetric mode, and the third was with excitation energy centered on the frequency of the first axi-symmetric mode.

Finally, samples were recorded for four cases of "broad band" excitation in which the bandwidth of the excitation was substantially increased over that for the "narrow band" excitation.

After completion of the actual data taking, color motion pictures were obtained of selected cases in the test program, and of a brief qualitative experiment to see if the first anti-symmetric mode could be excited in a substantial way with "narrow band" random excitation. The Appendix to this report contains notes and comments on these motion pictures.

DATA REDUCTION

All data reduction of the recorded samples was by the Hybrid-Analog-Digital methods outlined in the Section on Analysis Equipment.

The mean square measurements were carried out with a constant real time sampling interval, such that the <u>minimum</u> product: (sample time x effective energy bandwidth in the sample) was approximately 30. This implies a standard statistical error on <u>root mean square</u> estimates (Ref. 11) of approximately $\pm$ 10%, or in terms of a confidence statement for the root mean square values to be quoted: it may be said with about 90% confidence that the true rms value of the process is at worst within $\pm$ 15% of the estimate.

The choice of all analyzer bandwidths and integrating times for each spectral estimate was such as to make the product: analyzer bandwidth x sampling time equal to 60. This is equivalent to a standard error of about 13%, or, if the spectrum is "resolved" adequately, it may be said with about 90% confidence that the true spectral density is within $\pm$ 20% of the quoted estimate.

It is unfortunate that in order to adequately "resolve" a spectrum, it must be known in advance. In the present analyses a pilot analysis was carried out with a fairly broad effective analyzer filter bandwidth to determine where, in the frequency range, analysis with a narrower analyzer bandwidth should be carried out. On the basis of these analyses a second set of spectrum analyses was carried out to resolve peaks. The aim was to provide analyses where the analyzer bandwidth was 1/4 or less of the half power bandwidth of the spectral peak. In this, the second spectrum analysis was not entirely successful. However, in view of the exploratory nature of the program objectives, the use to be made of the spectra did not justify a third, more refined analysis. Of the results to be presented it is felt that the acceleration spectra are reasonably well resolved. For the most part the shape of these spectra were known in advance. On the other hand, since the present analyses of the spectra of free surface elevations in a tank may well be the first ever attempted, there was no good way to know in advance what sort of bandwidths to expect. Consequently, where relatively sharp spectral density peaks occur for free surface elevation, it should be assumed that the analysis procedure probably has distorted reality by lowering the maximum and broadening the bandwidth of the true spectral peak.

Cumulative probability distributions were estimated with the previously described equipment for selected samples in the test program. Since the basic noise source was Gaussian, the acceleration samples should have been

Gaussian. This was verified in one or two cases. Most of the samples selected for probability analyses were of fluid elevations, a response expected to be nonlinear and non-Gaussian. Each estimated point was plotted on normal probability paper as it was obtained, and where the total sample length on the magnetic tape allowed, some estimates were made in different portions of the recorded sample. These determinations of probability are effectively converted to the nominally equivalent standardized normal variate when plotted on normal probability paper. The scatter in the repeated determinations of the equivalent normal variate at a given level from different portions of the same sample typically scattered within 10-30% σ (σ = standard deviation of standard variate) depending on the estimated probability level. Since the statistical properties of the time intervals which make up the estimate $\hat{F}(E_o)$, Eq. 4, are not known for the non-Gaussian processes which were involved in the bulk of the analyses, and can only be approximated for a Gaussian process, confidence statements about the estimates cannot be made. On an intuitive basis, the sampling time, T , for all estimates was made the same and selected so that the length of record analyzed was equivalent to 400 times the period of the lowest period phenomena involved (the period of the first axi-symmetric mode). By analogy with digital sampling techniques, if the T seconds of recorded $X(t)$ had been sampled at an interval appropriate for digital analyses of the probability distributions in no case should the number of degrees of freedom (the number of statistically independent samples) have been less than 100. Thus, a respectable statistical sample, at least, is indicated.

RESULTS OF SPECTRUM ANALYSES

The results of the spectrum analyses will be presented and discussed approximately in the order of the experimental program, Table II.

1. Ultra Narrow Band Excitation

The applicable spectra are shown in Figures 8, 9, 10 for successively decreasing excitation level. In each figure, Acceleration Spectral Density in $g^2/\delta\Omega$ is denoted by $S_a(\Omega)$. Root mean square acceleration is denoted by $\hat{\sigma}_a$ and rms fluid elevation on the axis of symmetry by $\hat{\sigma}_\eta$. Spectral density of fluid elevation on the axis of symmetry is denoted by $S_\eta(\Omega)$, with units $(\text{diameter})^2/\delta\Omega$. All spectral estimates are plotted, even though those estimates 3 or 4 orders of magnitude below the highest peak in the analysis begin to be of marginal validity because of inherent signal to noise limitations of magnetic tape recording.

The "ultra narrow" band random excitation is the nearest approach to sinusoidal which was possible. It can be noted from the figures that the excitation spectrum is a "spike". Qualitatively, this type of excitation is a randomly modulated sine wave of frequency equal to twice that of the first axi-symmetric mode. The free surface visually fluctuated from almost negligible movement to very large amplitude, essentially first axi-symmetric mode response. Occasionally, the spike on the tank axis characteristic of this type of response would break up into globules, maximum vertical ascent of these globules was limited by the tank top (approximately 1.1 diameters above the nominal water level). It is clear from Figures 8-10 that the predominate response is at half the frequency of the excitation.

If the peaks of the fluid elevation spectra are compared in Figures 8-10 it can be seen that the variation in excitation level from 0.09 to 0.18 g's, rms had no great influence on the magnitude of the estimated peak spectral density. Though perhaps surprising in view of a previous assertion that the experimental variation in excitation level for this case would cover a transition range, it is not unusual for an experimenter making a decision on a small sample of a random process to be substantially in error. It is also not impossible in a random process as unusual as this one, that the amount of sample necessary to define the truth is substantially longer than that associated with the more common random processes encountered in practice. In effect, it is possible that the analysis of Figure 10 was carried out for a sample having an exceptionally high (statistically) level of activity. A third possibility is that some type of limit cycle is involved.

It may also be noted from Figures 8-10 that a consistent fluid elevation spectral density peak centered on the excitation was observed. This is analogous to harmonic excitation and since the spectral density is down two orders of magnitude in this frequency range the peak may be tentatively identified with the harmonic response observed under sinus-oidal excitation.

The only apparent differences between the fluid elevation spectra for this type of excitation is that as the excitation level decreases (Fig. 8 → 10) the contributions at frequencies <u>other</u> than Ω_{oo} or $2\Omega_{oo}$ decrease. It may be conjectured that the higher the excitation level, the more violent the breakup of the free surface. The collapse of exceptionally great vertical free surface excursions might be expected to produce a very wide spectrum of free surface motion.

To summarize the ultra narrow bandwidth experiments: 1/2 sub-harmonic response was definitely experienced but the rms acceleration level defining the onset of such response was not bracketed.

2. Very Narrow Band (1) Random Excitation

The results for this case are shown in Figures 11, 12, 13 for decreasing excitation levels. The excitation in Figs. 11-13 has a band-width 4 times as great as the excitation of the previous case. The results of the spectral analysis are essentially the same. Again, for excitation centered on twice the frequency of the first axi-symmetric mode, the response is at half the excitation frequency. "Harmonic" response is present for all three levels of excitation with about the same spectral density. The magnitude of spectral density for the subharmonic response is about the same as in the ultra narrow band case (Figs. 8-10). In this case, however, the spectral density at the "subharmonic frequency" (Ω_{oo}) drops by a factor of roughly 2 from the medium excitation level (Fig. 12) to the low excitation level (Fig. 13). As with the preceding case, activity at frequencies other than the excitation frequency or 1/2 this value decreases with decreasing excitation level.

3. Very Narrow Band (2) Excitation

Figures 14 and 15 are the applicable spectra. This case involves excitation bandwidths 4 times that of the preceding case, 16 times that of "ultra narrow" band excitation, but at the same frequency. The results are quantitatively and qualitatively the same. Subharmonic behavior was experienced but transition from harmonic to subharmonic behavior was not bracketed.

4. Narrow Band Excitation at Twice the First Axi-Symmetric Mode Frequency

Figures 16 and 17 are the results of the spectral analysis for this case which is for essentially the same type of excitation as for the preceding case except for a factor of 2 on excitation frequency bandwidth. The response spectrum in Figure 16 for the highest excitation level is essentially the same as that for the "very narrow" band case, Fig. 14. The rms excitation is the same for both figures. However, as the rms excitation level is reduced, Figure 17, the response changes significantly to predominately "harmonic". Subharmonic response is shown in Figure 15 for an excitation of the same rms level but half the bandwidth of that of Figure 17. Had a wider variation in excitation level been set, differences in spectral density of fluid response such as exist for this experimental case would probably have been experienced in all preceding narrower band excitation cases.

The similarity between fluid response spectra exhibited thus far for subharmonic behavior is striking. It is to be emphasized, however, that these are the spectra of fluid elevations on the tank axis, thus features of the spectra can only be identified with assumed axi-symmetric modes. Qualitatively, as the bandwidth of excitation increases, the large amplitude free surface behavior becomes "richer" in modal patterns. The present narrow band case (Fig. 16) has significant excitation energy from $\Omega = 6.2$ to $\Omega = 4.8$. The column of twice modal frequencies of Table I indicates that excitation of an $m = 2$, and an $m = 3$ mode would also be likely in this case. Qualitatively this is what was observed. Samples of this case are documented in the motion pictures. Figure 18 shows a number of photographs of the "narrow band" excitation situation. The $m = 2$ mode is apparently easier to excite than the $m = 3$ mode and is quite obvious in the figure in four of the eight photos. The figure illustrates the complexity of the free surface response for this case. The most spectacular large amplitude motion is a "spike" on the tank axis which shoots upward, occasionally, to about one tank diameter above the nominal fluid depth. Most of the pictures show only the collapse of this spike. The lower right-hand picture shows this in the clearest manner. The lower left-hand view shows the collapse of a spike on the tank axis (characteristic of the $m = 0$ mode) occurring simultaneously with a large amplitude $m = 2$ free surface mode.

5. The Influence of Center Frequency of Narrow Band Excitation

Qualitatively, as the center frequency of narrow band excitation as per Figure 16 was changed, maintaining the same rms acceleration level, the level and type of response on the tank axis went through maxima when

25

the excitation was centered on twice an axi-symmetric modal frequency.
Figure 19, for the case where the excitation was centered on the first
axi-symmetric modal frequency, indicates typical harmonic response.
Figures 20 and 21 show the results of cases where the excitation was
centered on twice the second and third modal frequencies, respectively.
In both cases, subharmonic response in the appropriate higher axi-
symmetric modes is exhibited as would be expected. The resolution of
the spectra is too coarse but there is some indication that the higher
"modes" are coupled to adjacent lower "modes".

6. "Broad Band" Excitation Results

The results of the first case are summarized in Figure 22. In
this case the excitation was "white" with respect to the first 15 or 20
axi-symmetric modal frequencies (with respect to the first 150 or so free
surface modes). Because of shaker limitations, the excitation level was
not high enough to make anything much happen. It may be that the approxi-
mate factor of two between the high frequency "shoulders" of excitation
and response spectra means that the higher mode response is subharmonic.
However, not much can be made of this since the faster "rolloff" of the
response spectrum may also imply simply that high axi-symmetric modes
are difficult to excite in any way.

The results of a second case of broad band excitation are shown
in Figures 23 and 24. In this case, the passband was adjusted so that
the excitation energy content at the first axi-symmetric mode was about
1/50 that at twice this frequency. The response spectrum of Figure 23 has
the typical shape and magnitude of those exhibited previously for subharmonic
response to narrow band excitation. In contrast, the spectra in Figure 24
indicate only harmonic response in the lowest axi-symmetric mode. It
should be emphasized that the difference in excitation between the experi-
ments of Figures 23 and 24 is only in excitation level. The excitation
spectrum shapes are the same, the rms acceleration for the case of
Figure 24 is only 2/3 that for the case of Figure 23. Thus even in the
case of broad band excitation an abrupt transition between harmonic and
subharmonic response is indicated.

In Figure 24 the peaks of the fluid response spectra are in the vicinity
of the 3rd to 5th axi-symmetric modes. Since significant energy is present
in the excitation at both the frequency range of these modes and at double
this range, the response in Figure 24 cannot be directly identified as harmonic
or subharmonic. However, to produce the last case of broad band excitation,

Figure 25, the low frequency rolloff of Figure 24 was essentially raised an octave in frequency. Thus the excitation energy content at <u>twice</u> the frequency range of the 3rd-5th axi-symmetric mode is about the same in Figure 25 as in Figure 24 but the excitation content <u>in</u> this modal frequency range is significantly reduced. It may be noted by comparing Figures 24 and 25 that the fluid response near the 3rd-5th modal frequencies is also significantly reduced, thus indicating that it is "harmonic" in nature in Figure 24.

DISCUSSION OF RESULTS

The primary question under investigation herein was phrased in the preliminary discussion to this report as: Is <u>Large Amplitude</u> <u>Free Surface Motion Response to Random Excitation Qualitatively</u> Similar to the '1/2 Subharmonic Response' Observed in Sinusoidal Experiments...?" Insofar as the limitations on an exploratory program will allow generalizations, the answer seems to be "yes".

In the experimental program the point of the ultra narrow" band excitation condition was to provide as close as possible an analogy to sinusoidal excitation so that the necessarily different type of results could be related to past sinusoidal excitation experiments. To come to the conclusion that the large amplitude response was "1/2 subharmonic" in nature, a spectrum analysis was hardly necessary in this case. Because of the high purity of the excitation, simple visual monitoring of the excitation and response during the experiment made it clear that the apparent frequency of large amplitude response was half that of the excitation. Though, unfortunately, data was not obtained in substantiation, there was a level of ultra narrow band excitation below which the fluid response was at the <u>same</u> apparent frequency as the excitation. Thus, the spectral analyses for the ultra narrow band excitation case can, in a sense, be considered as an empirical "translation" of sinusoidal excitation experience into a form more suitable for the description of random excitation results. The spectral results of ultra narrow band random excitation are strikingly similar to the fluid response spectra in the experiments involving large amplitude fluid response to <u>wider</u> band excitation. In all cases, a very low level harmonic response is involved, exactly as in sinusoidal excitation experiments. When the random excitation contained enough energy at twice the modal frequency of higher axi-symmetric modes, these modes were apparently excited at large amplitude. The results from observation of the entire free surface (as opposed to measurements on the tank axis) indicate that so long as enough excitation energy is provided at double the applicable frequency, modes which are adjacent in frequency, regardless of type (anti-symmetric, axi-symmetric, $m = 2, 3, 4....$) may be excited into <u>simul-taneous</u> large amplitude "1/2 subharmonic" behavior. Qualitative experiments on the important (for stability and control) first anti-symmetric mode were carried out but are documented only in motion pictures. Qualitatively, fluid response in this mode to random excitation may be expected to be identical to that of the first axi-symmetric mode.

Beyond the question of the existence of fluid response analogous to that observed in sinusoidal excitation, there is the quantitative question of what circumstances are necessary to produce the large amplitude response

under random excitation. For sinusoidal excitation the conditions can be expressed as a stability chart similar to Figure 7. In this figure for excitation levels below the line, low level essentially harmonic response is expected, while above the line essentially large amplitude subharmonic response is expected. For a beginning at correlating, all the rms excitations and responses were plotted in Figure 26, where rms fluid response is the ordinate and rms acceleration the abcissa. Judging by the spectrum analyses any rms fluid response above about .01 to .02 diameters, rms is subharmonic. If the results of a sinusoidal experiment where acceleration amplitude was varied upward were plotted on Figure 26 an abrupt "jump" in plotted rms fluid response should occur at an rms acceleration near the line on the stability chart, Fig. 7. From Figure 7 the value of this transition acceleration for sinusoidal excitation at twice the first axisymmetric mode frequency might be between 0.075 and 0.15 g's rms. (The stability boundary is very steep in this region of frequency, small differences in excitation frequency result in large differences in position of the boundary.) In Figure 26 the points connected by lines involve significant excitation at twice the first axi-symmetric modal frequency and it may be seen that the tendency is for the fluid response to narrow band excitation to change from harmonic to subharmonic behavior in the acceleration "ball park" predicted from Figure 7. The lines for the different excitation bandwidths suggest a "family" having some consistent relationship. It is to be noted that transition between harmonic and subharmonic behavior in the first axi-symmetric mode is between 0.25 and 0.35 g's rms for the broad band excitation case where the excitation bandwidth, $\Delta\Omega$, was 12 (Figures 23 and 24, the applicable points on Figure 26 are referenced to these figures). The points on Figure 26 represented by large circles containing a figure number correspond to the special narrow band excitation tests of Figures 19-21. The two of these points near an rms acceleration of 0.3 g pertain to subharmonic response in higher axi-symmetric modes. These modes, under sinusoidal excitation would be expected to be large amplitude subharmonic at an rms acceleration less than 0.1g.

The results depicted in Figure 26 simply demonstrate the obvious: the conditions for a "1/2 subharmonic" type response to random excitation involve both the level and frequency distribution of excitation energy. As random excitation becomes more nearly analogous to sinusoidal (by decreasing the frequency band) the value of random rms acceleration for transition from harmonic to subharmonic grossly approximates that of sinusoidal rms acceleration for a similar transition.

A plausible parameter to use in predicting the possibility of 1/2 subharmonic response might be the spectral density of acceleration. The results of an attempt to correlate acceleration spectral density and type of

free surface response is shown in Figure 27. It was observed in the spectral analyses that the peak fluid response spectral density in cases where the response was judged subharmonic was greater than 0.0001 $(dia)^2/\delta\Omega$, those peaks for "harmonic" response were less. Accordingly, the peak fluid response spectral density is plotted in Figure 27 vs. the acceleration spectral density at twice the frequency of the peak fluid response spectral density. Results from experiments where the response was judged subharmonic are identified by the letter "S". There appears to be a value of acceleration spectral density defining the transition between harmonic and subharmonic response. The starred points (S^*) are from the experiments involving higher axi-symmetric modes than the first. Since the higher modes are more difficult to excite, these points should perhaps not be considered in conjunction with the rest. The fragmentary results in Figure 27 may imply that the conditions for large amplitude subharmonic response to random excitation may possibly be stated in a diagram similar to Figure 7 wherein a transition acceleration spectral density would be plotted as a function of frequency.

ESTIMATES OF THE PROBABILITY DISTRIBUTION
OF FREE SURFACE ELEVATION

The probability structure of the large amplitude free surface response might be of potential importance from the engineering viewpoint and central to theoretical investigations. Consequently, distributions of selected responses were estimated using previously described equipment and procedures. The excitation in the present experiments was normally distributed, Figure 28 is a typical result for the distribution of acceleration. (Cumulative distributions estimated from samples of normally distributed processes should plot as straight lines on the type of paper used in Fig. 28.)

Of the 17 available samples of fluid elevation, 8 were selected for probability distribution analysis as in Table III.

TABLE III. Conditions Selected for Probability Analysis

Type of Excitation	rms Acceleration g's	Spectrum Figure No.	Type of Response (from Spectrum Analyses)
Ultra Narrow Band	0.184	8	Subharmonic
Very Narrow Band (1)	0.17	11	"
Very Narrow Band (1)	0.086	13	"
Very Narrow Band (2)	0.191	14	"
Narrow Band	0.190	16	"
Narrow Band	0.124	17	Harmonic
Broadband	0.366	23	Subharmonic

As the estimates were made and plotted on normal probability paper it was immediately apparent that all except one of those samples chosen for analysis were probably not normally distributed. Later analysis showed that the one sample which appeared approximately normally distributed was the case in Table III adjudged "harmonic". All the estimates from samples adjudged "subharmonic" displayed the same characteristics when plotted on normal probability paper. All the elevations η_o corresponding to the probability estimate $\hat{F}(\eta_o)$ were normalized by division by the sample rms elevation σ_η. It was found that almost all the estimates then plotted within a relatively narrow band on normal probability paper, Fig. 29. (The

exceptions were points from the sample of "harmonic" response.)
Referring to Fig. 29, if the distributions involved were normal the band
shown would be expected to be more or less centered on the straight line
labeled "normal distribution," or about a parallel line. While estimates
from a sample of almost any continuous distribution would be close to a
straight line between the probability levels 0.25 and 0.50, large, consistent
deviations in the "tails" of the distribution such as are shown in Fig. 29
strongly indicate non-normality (Ref. 12, 13). Again, within the limita-
tions of an exploratory program, the analysis indirectly indicates that
the large amplitude response is "1/2 subharmonic". Since this is a sub-
stantially nonlinear random response by definition, a normal distribution
is not to be expected.

Since the data for the "subharmonic" samples lay in a relatively
narrow band (Fig. 29) when normalized by the sample variance, it was
felt of potential interest to attempt to describe this band by some fitting
procedure and thus to be in a position to describe the apparent distribution
by means of the conventional moments (mean, variance, skewness, etc.).

An estimate for the mean $(\bar{\eta})$ of each distribution was obtained
by assuming that the centroid of the unknown density function $f(\eta)$
included between two successive point estimates of the cumulative prob-
ability $\hat{F}(\eta_i)$ and $\hat{F}(\eta_{i+1})$ was located midway between the levels
η_i and η_{i+1}. The results were examined in the light of remarks
on such methods in Ref. 12, pp. 361 and felt to be reasonable. Having
estimates for the mean and the sample variance $\hat{\sigma}_\eta$, the fluid elevation
levels η_i corresponding to each probability estimate $\hat{F}(\eta_i)$ were
transformed into the standardized form for the normal distribution:

$$X \quad = \text{ standardized normal variate}$$

$$= \frac{\eta_i - \bar{\eta}}{\hat{\sigma}_\eta}$$

where

$$\eta_i \quad = \text{ fluid elevation}$$

$$\bar{\eta} \quad = \text{ estimated mean fluid elevation}$$

$$\hat{\sigma}_\eta \quad = \text{ rms fluid elevation from spectrum analyses.}$$

A re-plot of the transformed cumulative probability $\hat{F}(X)$ on normal
probability paper showed somethat more compression of the data than
is shown in Fig. 29.

It was felt that estimates of the third and higher moments using the same general procedure as for the mean was inadvisable. Consequently, an attempt was made to fit the cumulative probability data by means of an Edgeworth asymptotic expansion, Ref. 12, pp. 229. However, by the time that it was found that third and possibly higher order terms in the expansion would have to be retained for a reasonable fit, an alternate approximation was happened upon.

It was noted in Ref. 12 that the shape of an extreme value distribution used therein when plotted on normal probability paper was very similar to that of the estimated cumulative distributions of free surface elevations, Fig. 29. The extreme value distribution involved is sometimes called the doubly exponential distribution and is an asymptotic expansion of the distribution of the largest among a number of independent observations from a population having an exponential class distribution. However, since the distribution was hoped to be an aid to <u>description</u>, its origin was ignored.

The doubly exponential distribution is defined as

$$F(Y) = \text{cumulative probability}$$

$$= e^{-e^{-Y}}$$

$$f(Y) = \frac{d}{dY} F(Y) = e^{(-Y - e^{-Y})}$$

$$= \text{probability density.}$$

where the variate Y may be written:

$$Y = \frac{\pi}{\sqrt{6}} X + \gamma$$

$$\gamma = \text{Euler's constant}$$

$$= 0.577215665$$

$$X = \text{standardized variate,} \quad \frac{\eta - \bar{\eta}}{\hat{\sigma}_\eta}$$

A least square fit of the raw probability estimates to this cumulative distribution was made, and the resulting estimated mean value and sample variances by this method were compared with those previously estimated. The correspondence of means and variances was good.

Since the standardized normal variate and the variate Y in the doubly exponential distribution are linearly related, the estimated cumulative probability $\hat{F}(X)$ may be plotted on extreme value probability paper for the doubly exponential distribution with the expectation that if the actual underlying distribution is doubly exponential the estimates will lie on a straight line.

This procedure was followed for the estimates from the cases detailed in Table III and the results are exhibited as Figures 30-32. In Figure 30 data from 5 of the 7 samples are shown. These five samples were all judged "subharmonic" and were obtained at the highest excitation level. The lines on the plot are for the doubly exponential distribution and the normal distribution. It is clear that the general trend of the estimates is along the doubly exponential distribution. If the point estimates for each sample were connected by lines it would be clear that the estimates do not lie on straight lines. If the statistics of the present estimates of cumulative probability were known, it might be possible to estimate whether or not the scatter shown would be expected considering sample size, etc. This effort would be rather a nightmare and could not be attempted within the limitations of an exploratory project. The answer sought in this exercise was a gross description of what was observed. The doubly exponential distribution is one of hundreds which might be reality and is offered here as a potential starting point for a careful investigation.

Figure 31 shows the free surface distributions for Very Narrow (1) excitation at two rms excitation levels. Both samples are adjudged "subharmonic" and the general trends agree. Figure 32 shows the estimates for "Narrow Band" excitation at two rms acceleration levels. The fluid response was adjudged "subharmonic" for the higher level and "harmonic" for the lower. The two estimated points for the lower level excitation at probability levels around 0.998 are quite significantly different than the doubly exponential distribution, in relation to the repeatability of the basic estimating methods, and, owing to the proximity to the normal distribution of the estimates, it may be tentatively hypothesized that "harmonic" fluid response is approximately normally distributed.

For visualization of the possible differences between the probability structure of "harmonic" and "subharmonic" response, Figure 33 shows a graphical comparison of the normal and doubly exponential distribution. Figure 34 is a plot of the doubly exponential distribution to a base of fluid elevations rather than the standardized variates utilized in the previous figures.

CONCLUDING REMARKS

At the outset of the investigation it was not known if significant large amplitude free surface response could be excited by random longitudinal excitation. There is no doubt in the author's mind that it can. Moreover, within the range of excitation parameters utilized in the experiments, very strong indications were found that when large amplitude response is excited, it is of the "1/2 subharmonic" nature predicted and observed under harmonic excitation. The tentative hypothesis is advanced that it may be possible to demonstrate that the onset of large amplitude response to longitudinal random accelerations may be predicted on the basis of spectral density of the excitation in a manner analogous to the stability diagram derived for harmonic excitation.

An even more tenuous hypothesis is advanced that low level harmonic response to random Gaussian excitation is nearly Gaussian, but that when large amplitude "subharmonic" response is excited the probability structure changes abruptly into something approaching a doubly exponential distribution.

It should be remarked that considerable additional analytical work must be accomplished if productive future work on this subject is to be visualized. The present experiments were a "stab in the dark" in the absence of a suitable theoretical background for general (as opposed to harmonic) longitudinal excitation.

ACKNOWLEDGEMENTS

REFERENCES

1. H. Norman Abramson (Editor), THE DYNAMIC BEHAVIOR OF LIQUIDS IN MOVING CONTAINERS, NASA SP-106, Contract NASr-94(07), Southwest Research Institute, 1966.

2. John F. Dalzell, "Exploratory Studies of Liquid Behavior in Randomly Excited Tanks: Lateral Excitation," Tech. Rept. No. 2, Contract NAS8-20319, Southwest Research Institute, May 1967.

3. D. D. Kana, U. S. Lindholm, and H. N. Abramson, "An Experimental Study of Liquid Instability in a Vibrating Elastic Tank," AIAA Symposium on Structural Dynamics and Aeroelasticity, pp. 162-168, Boston, August 1965; also, AIAA Journal of Spacecraft and Rockets, Vol. 3, No. 8, pp. 1183-1188, August 1966.

4. Wen-Hwa Chu and D. D. Kana, "A Theory for Nonlinear Transverse Vibrations of a Partially Filled Elastic Tank," Final Report, Part I, Project 02-1748(IR), Southwest Research Institute, March 1966. Presented AIAA Fifth Aerospace Sciences Meeting, January 1967. To appear, AIAA Journal.

5. D. D. Kana, "Parametric Coupling in a Nonlinear Electromechanical System," Final Report, Part II, Project 02-1748(IR), Southwest Research Institute, May 1966. Presented, ASME Vibrations Conference, Boston, March 1967. To appear in Journal of Machine Design.

6. D. D. Kana, "Longitudinal Dynamics of Liquid Filled Elastic Shells," Summary Report, Contract NAS8-11045, September 30, 1965.

7. D. D. Kana, "Bubble Dynamics in Vibrated Liquids Under a Low Gravity Environment," Technical Report No. 8, Contract No. NAS8-11045, 15 February 1967.

8. C. R. Gerlach, "Surface Instability and Disintegration of Liquid in a Longitudinally Excited Container," Tech. Rept. No. 9, Contract No. NAS8-11045, 15 March 1967.

9. Franklin T. Dodge, Daniel D. Kana, H. Norman Abramson, "Liquid Surface Oscillations in Longitudinally Excited Rigid Cylindrical Containers," Tech. Rept. No. 2, Contract No. NAS8-11045, 30 April 1964. Also, AIAA J., Vol. 3, No. 4, April 1965, pp. 685-695.

10. John F. Dalzell, "Notes on the Discrimination of Free-Surface Modes in a Cylindrical Tank," Tech. Rept. No. 3, Contract NAS8-20319, Southwest Research Institute, May 1967.

11. Julius S. Bendat and Allan G. Piersol, Measurement and Analysis of Random Data, John Wiley & Sons, Inc., New York, 1966.

12. Harald Cramer, Mathematical Methods of Statistics, Princeton University Press, 1946.

13. Emil J. Gumbel, "Statistical Theory of Extreme Values and Some Practical Applications," National Bureau of Standards Applied Mathematics Series 33, February 12, 1954.

APPENDIX

NOTES ON:

EXPLORATORY STUDIES OF LIQUID BEHAVIOR
IN RANDOMLY EXCITED TANKS:
LONGITUDINAL EXCITATION

Motion Picture Report No. 1
Contract No. NAS8-20319
Control No. DCN 1-6-57-01042(1F)

TYPE FILM: Silent - Color

PROJECTION TIME: Approximately 20 minutes at 16 frames/sec.

GENERAL: Sequences showing the tank in motion were framed so that the tank fills up the picture and only the gray top of the shaker (Figure 2 of this report) is visible. All sequences were taken at 32 frames per second so that the time scale, when the film is projected at 16 frames, is appropriate for an 18 inch (45.6 cm) tank in a 1 g acceleration field.

COMMENTS ON THE FILM SEQUENCES

a. After identification titles, two sequences are shown of sinusoidal excitation. The first is sinusoidal excitation of about 0.2 g's rms and a frequency equal to that of the first axi-symmetric mode. Harmonic response is present under these conditions but visually nearly indistinguishable. The second sinusoidal excitation sequence involves excitation of about the same amplitude but of a frequency twice that of the first axi-symmetric mode. A typical "1/2 subharmonic" response in the first axi-symmetric mode is shown.

b. The next sequence involves "ultra narrow band" random excitation, half power band about 0.04, 0.18 g's, rms, centered on twice the frequency of the first axi-symmetric mode. A chart showing the relation between spectral densities

A-1

is shown. This excitation is qualitatively a <u>randomly</u> <u>modulated</u> sine wave. Its spectrum is almost a line in the chart. The spectrum of the free surface elevation on the axis of symmetry (in red) has its predominate energy at 1/2 the excitation center frequency. The sequence of the run itself, which follows, shows "1/2 subharmonic" response in the first axi-symmetric mode with little or no visible response in other modes. It is characteristic of the excitation level to fluctuate and so the visible response varies from nil to very large amplitudes, occasionally with break-up into droplets.

c.   The sequence which follows shows "very narrow band" random excitation. This excitation is essentially the same as that preceding except that the excitation half power band is 4 times as great. A chart is shown of the spectral densities, showing the same relative locations of "input" and response energies as in the previous case and the sequence of the run itself is qualitatively almost indistinguishable from that preceding for "ultra narrow band" excitation.

d.   An additional factor of eight in excitation half power bandwidth is involved in "narrow band" random excitation which follows. The excitation level is about the same as in the previous runs (0.19 g's, rms) and the excitation is centered on twice the first axi-symmetric mode. The chart again shows predominate response energy at half the excitation center frequency. The run itself, which follows, shows a somewhat reduced response in the first axi-symmetric mode, and for the first time in the motion picture, significant response in other modes adjacent in frequency to the first axi-symmetric, ($m=0$, $n=0$). The ($m=2$, $n=0$) mode is particularly pronounced, it is the next lower mode in frequency to the first axi-symmetric. In multiple reviews of this sequence, the reviewer suspected some significant ($m=3$, $n=0$) mode (the next higher mode in frequency) and a suggestion of the first anti-symmetric mode ($m=1$, $n=0$).

e.   The sequences following outline a sample of "broad band" excitation. In this case the excitation level was about double that of the preceding sequence, (0.37 g's rms) but the half power band was eight or ten times as great as in the immediately

preceding run. As the chart shows, significant excitation energy was not present at the frequency of the first axi-symmetric mode, yet most of the energy in the free surface elevation occurred at this frequency. The sequence showing the run itself shows long periods of calm punctuated by occasional response in the first axi-symmetric ($m=0$) mode and in the adjacent ($m=2$) mode.

f. The case following shows a return to "narrow band" excitation, this time showing that excitation centered on twice the frequency of the second axi-symmetric mode results in significant energy content in that mode. A chart is shown showing the spectral densities. Qualitatively, the photographs of the tank show response in the second axi-symmetric mode ($m=0, n=1$) as well as in the adjacent (in frequency) $m=2$ and $m=3$ modes. An $m=6$ mode, just above the second axi-symmetric mode in frequency, is not obviously excited, but may in fact be obscured by the general level of violence in the response.

g. The last two sequences in the motion picture involve a qualitative study of the excitation of the first anti-symmetric mode. The first part of this sequence shows sinusoidal excitation at twice the frequency of the first anti-symmetric mode. A well developed "1/2 subharmonic" response in the first anti-symmetric mode is observed, without significant rotation. The next (and last) sequence in the motion picture is of "narrow band" random excitation centered on twice the frequency of the first anti-symmetric mode. Qualitatively, the response here is very much what might have been expected from the work on 1/2 subharmonic axi-symmetric mode excitation. Pronounced anti-symmetric mode response is evident, without rotation, and some suggestion of response in modes immediately adjacent in frequency ($m=2$ and $m=0$) can be observed.
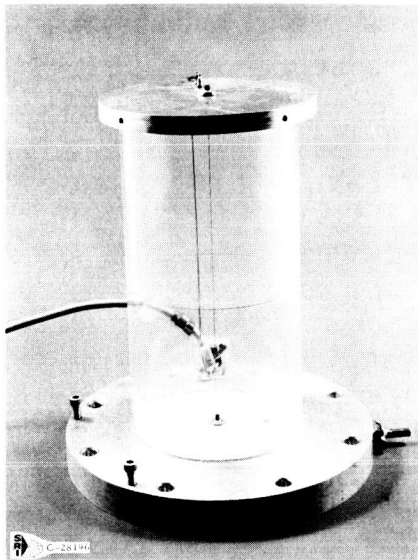
Figure 1. Test Tank With Surface Elevation Probe
On Axis Of Symmetry
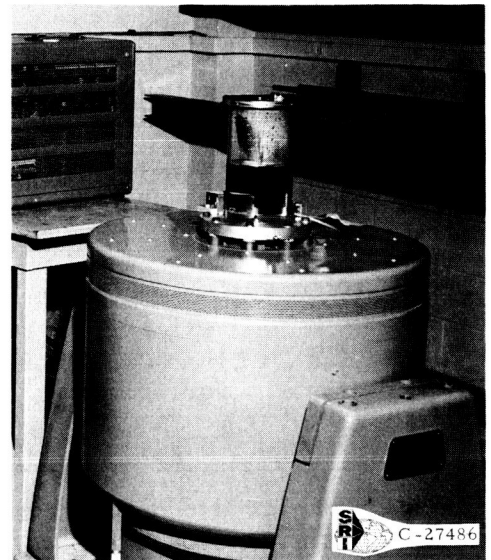
Figure 2. Tank And Shaker
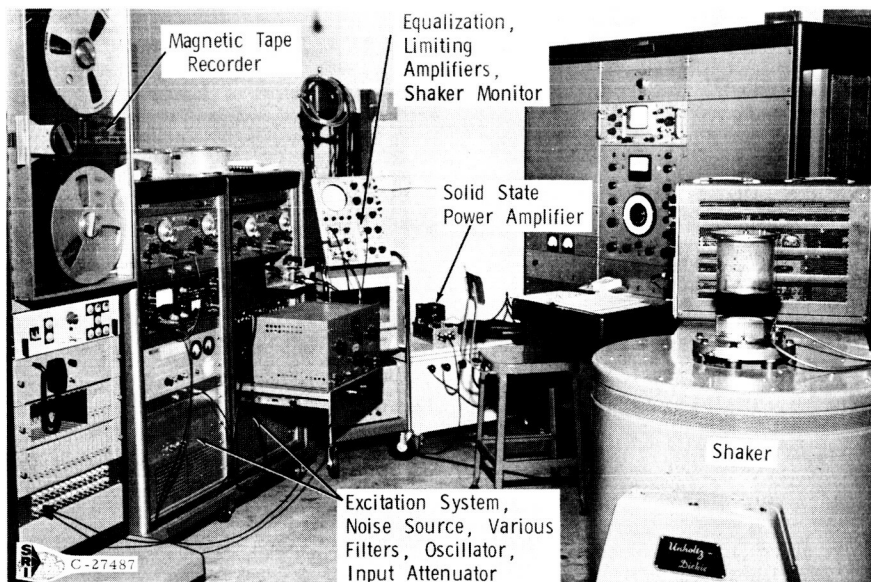
Figure 3. Electro Mechanical Setup

BLOCK DIAGRAM   FUNCTION AND REMARKS

| Hewlett Packard Voltage Calibrator | | Ampex FR 1800L Magnetic Tape Recorder (Tape Speed V_t) |

Data Recorded at Speed V_r, Played Back at Speed V_t

$$\frac{V_r}{V_t}(t) = \frac{\text{Apparent Time}}{\text{Real Time}} = N(t)$$

1 V. RMS Calibration as Required

X(Nt), Random Data Under Analysis in Compressed Time Scale

| Spectral Dynamics Sweep Oscillator | f → | Spectral Dynamics Tracking Filter; Effective Bandwidth B_e (B_e = 2 or 20 cps) |

X(Nt), Filtered by Narrow Bandpass Filter of Effective Width B_e and Center Frequency (f)

X(Nt, f, B_e), Filtered Signal

Manual Adjustment of f

| Ballantine True RMS Voltmeter; Attenuator A Square Law Output |

Squaring of Attenuated, Filtered Signal, Attenuator Adjustment as Required for Readout Requires Later Multiplication of Readout by q (A)

X^2(Nt, f, B_e)/q (A), Squared Filtered Signal

| Digital Voltmeter; Input Stages and Voltage to Frequency Converter Only |

Essentially a Voltage to Frequency Converter

X^2(Nt, f, B_e)/q (A) (Frequency Modulated)

| Gate Time Oscillator | f_T → | Hewlett-Packard Digital Counter; Manual Start— Gated Stop After K_t Cycles of f_T |

Sample Time $T = \dfrac{K_T}{f_t}$ Sec.

Accumulated Count of Cycles of FM Signal Input

Digital Display

Count Accumulated in Sample Time T is Closely Proportional to:

$$\frac{1}{q(A)} \int_0^T X^2(Nt, f, B_e)\, dt$$

Figure 4. Spectrum Analyzer Block Diagram
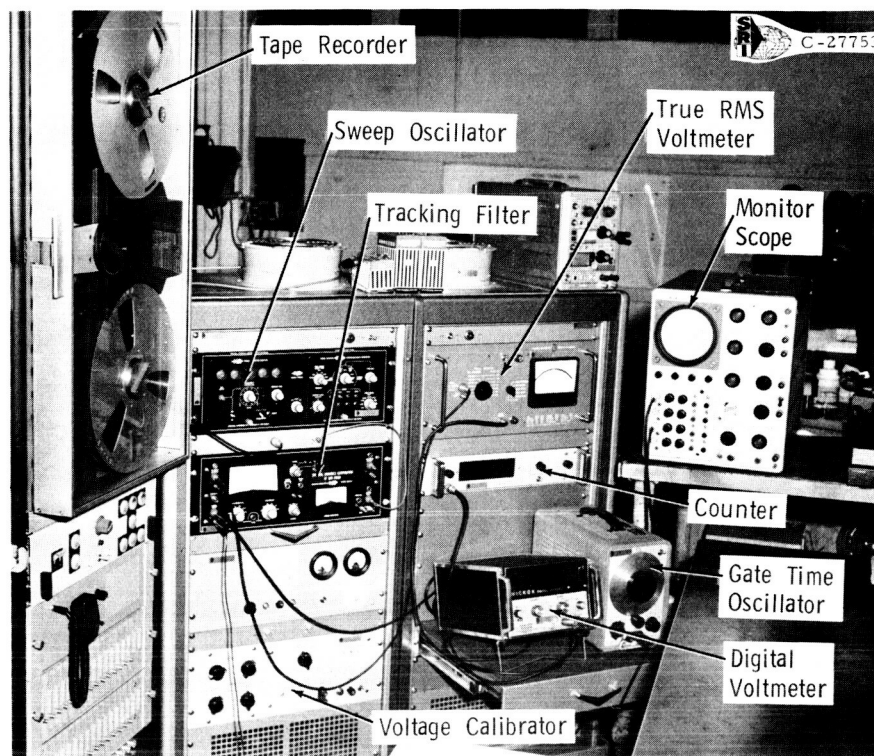
Figure 5. Spectrum Analysis Equipment
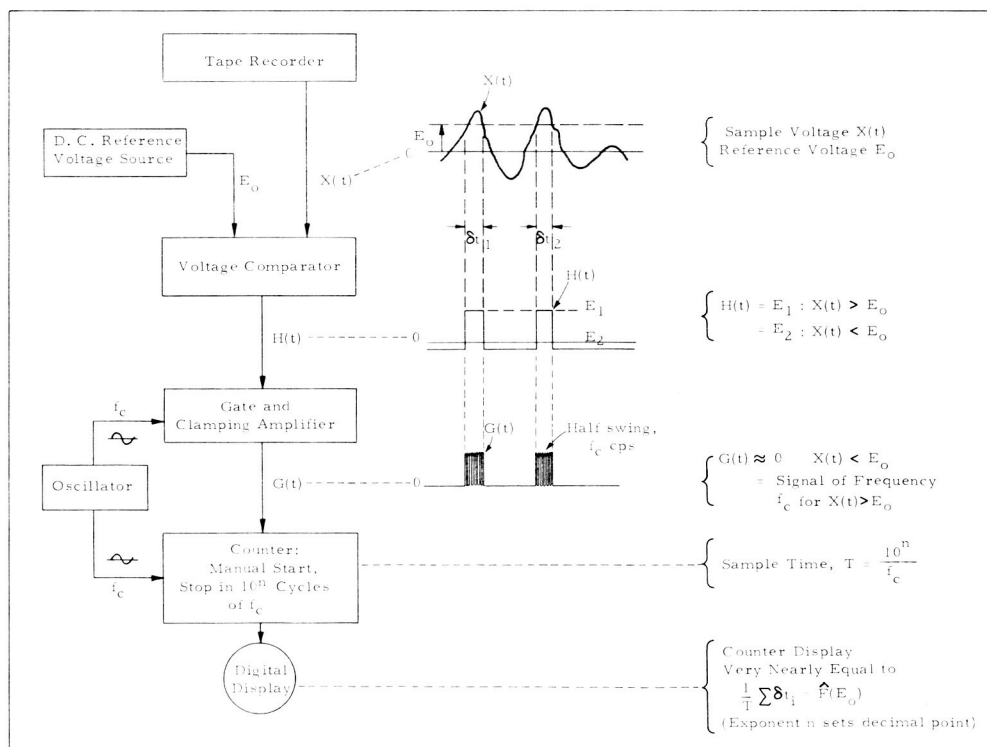
Figure 6. Block Diagram – Probability Distribution Estimation
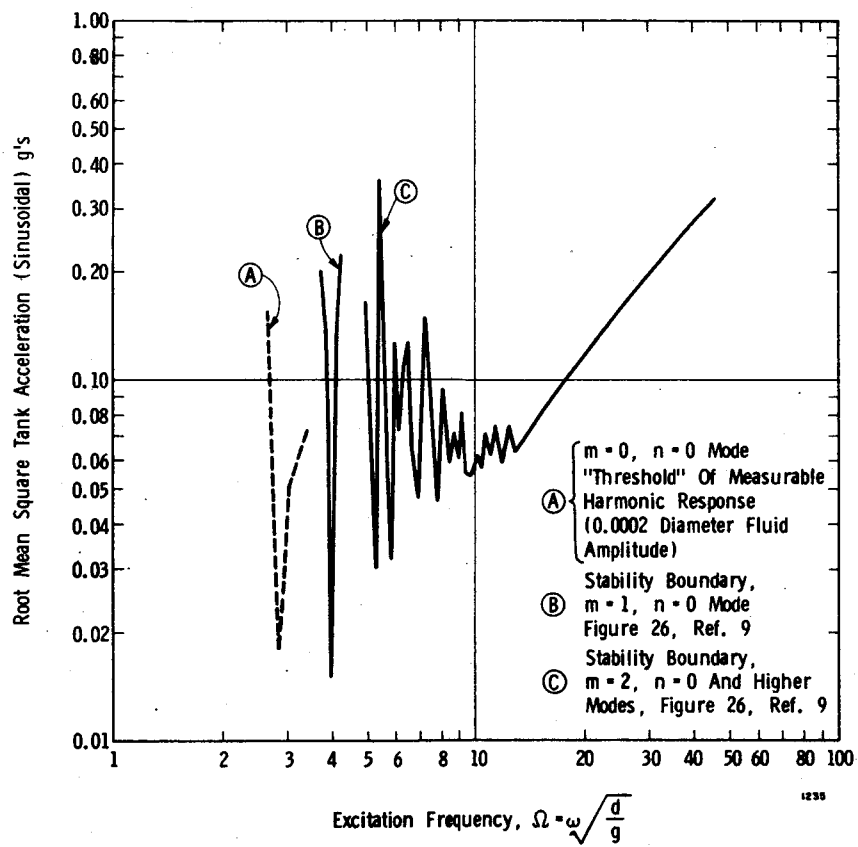
Figure 7. Stability Boundaries

$2\,\Omega_{oo}$

Ω_{oo}

$S_\eta(\Omega)$
$\hat{\sigma}_\eta = 0.10$ Dia.

$S_a(\Omega)$
$\hat{\sigma}_a = 0.184$ g's
$\Delta\Omega = 0.04$

Ω_{oi}

$S_\eta(\Omega)$, (Diameter)$^2/\delta\Omega$

$S_a(\Omega)$, g$^2/\delta\Omega$

Frequency, Ω

1237
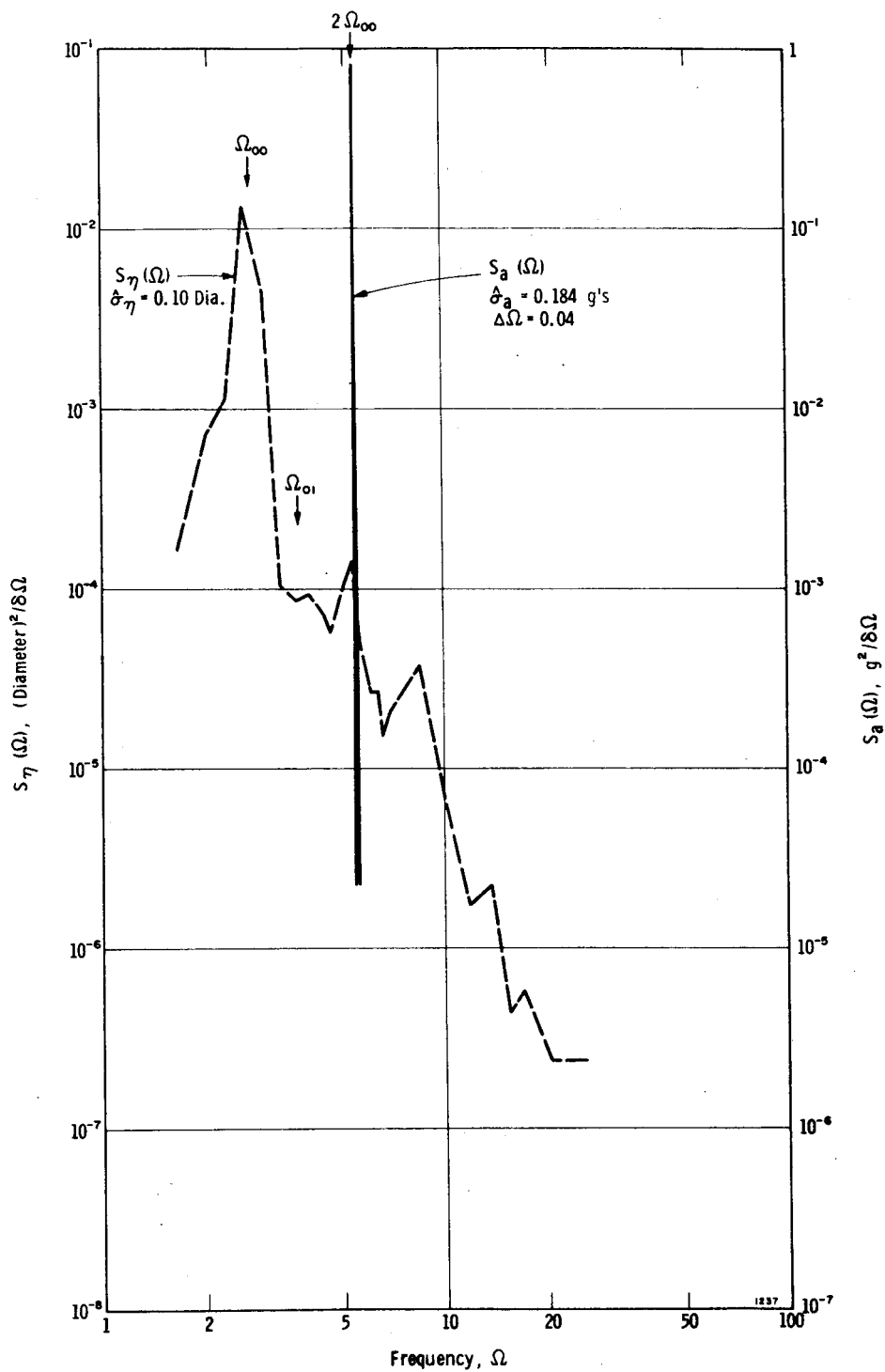
Figure 8. Spectra: Ultra Narrow Band Random Excitation,
Maximum Excitation Level
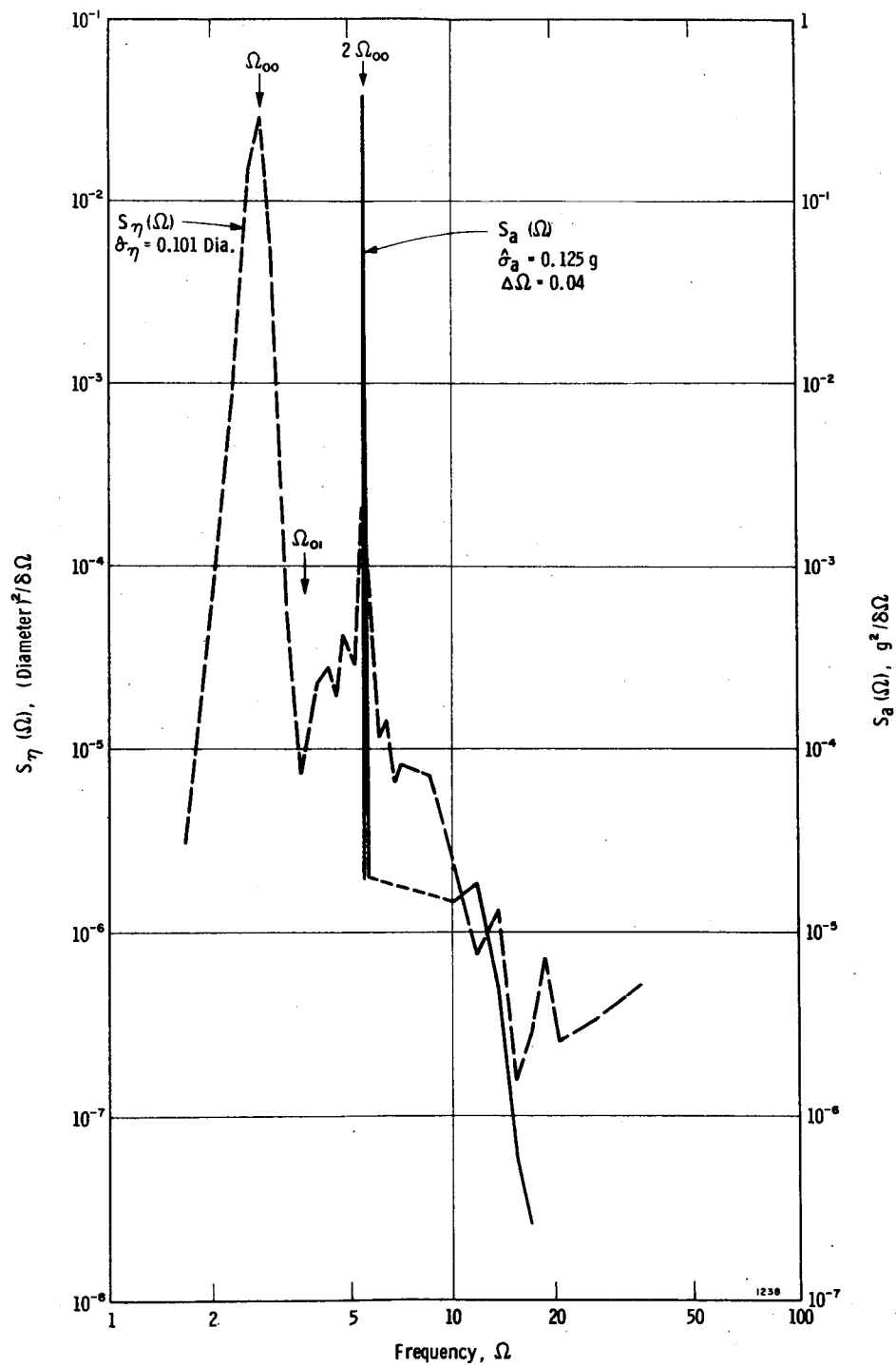
Figure 9.   Spectra: Ultra Narrow Band Random Excitation,
Medium Excitation Level
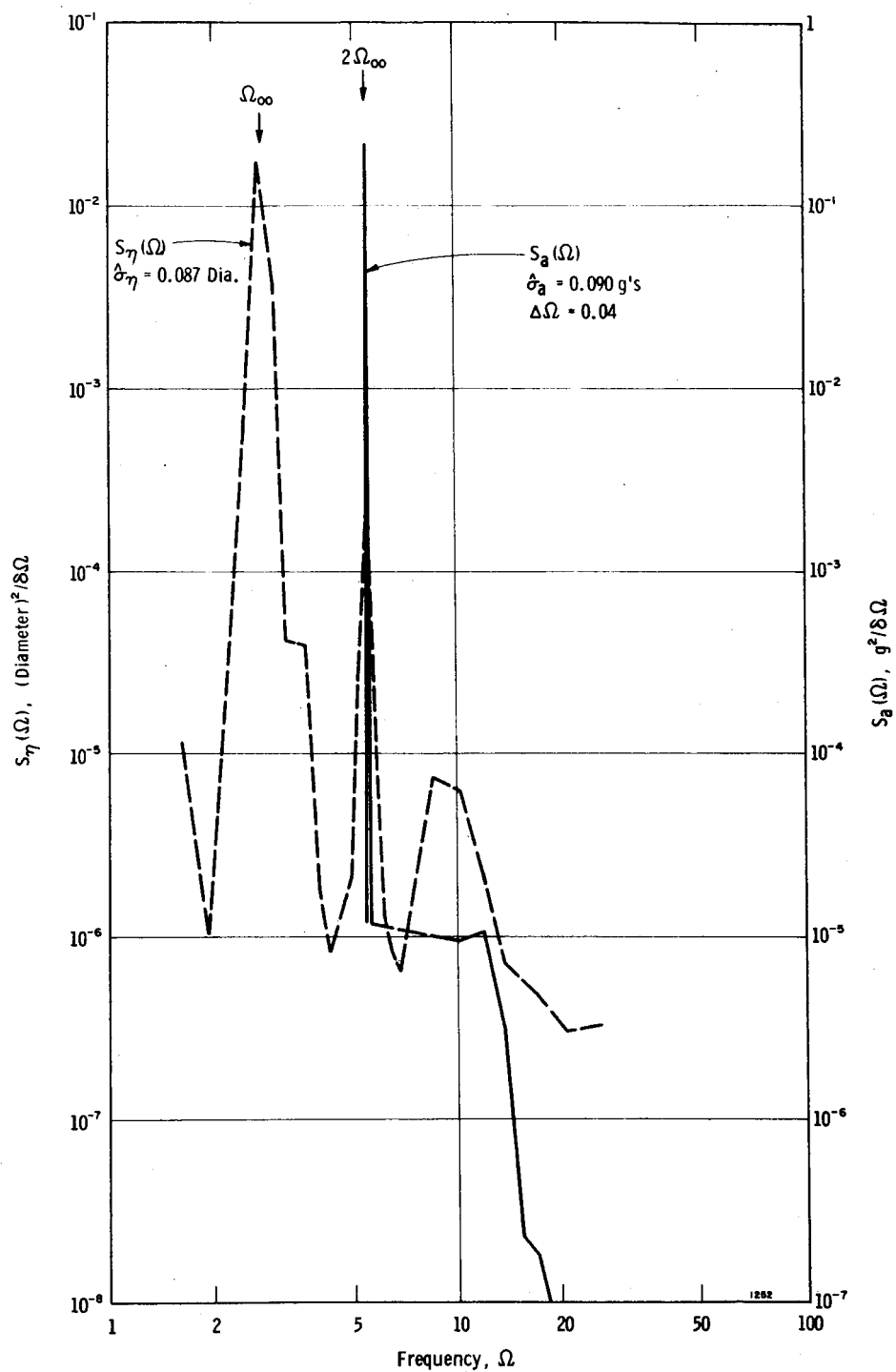
Figure 10. Spectra: Ultra Narrow Band Random Excitation,
Low Excitation Level

Ω_{oo}

$2\Omega_{oo}$

$S_\eta (\Omega)$
$\hat{\sigma}_\eta = 0.10\,Dia.$

$S_a (\Omega)$
$\hat{\sigma}_a = 0.167\,g$
$\Delta\Omega = 0.17$

10^{-1}
10^{-2}
10^{-3}
10^{-4}
10^{-5}
10^{-6}
10^{-7}
10^{-8}

1
10^{-1}
10^{-2}
10^{-3}
10^{-4}
10^{-5}
10^{-6}
10^{-7}

$S_\eta (\Omega)$, (Diameter$)^2/\delta\Omega$

$S_a (\Omega)$, $g^2/\delta\Omega$

1   2   5   10   20   50   100

Frequency, Ω

1250
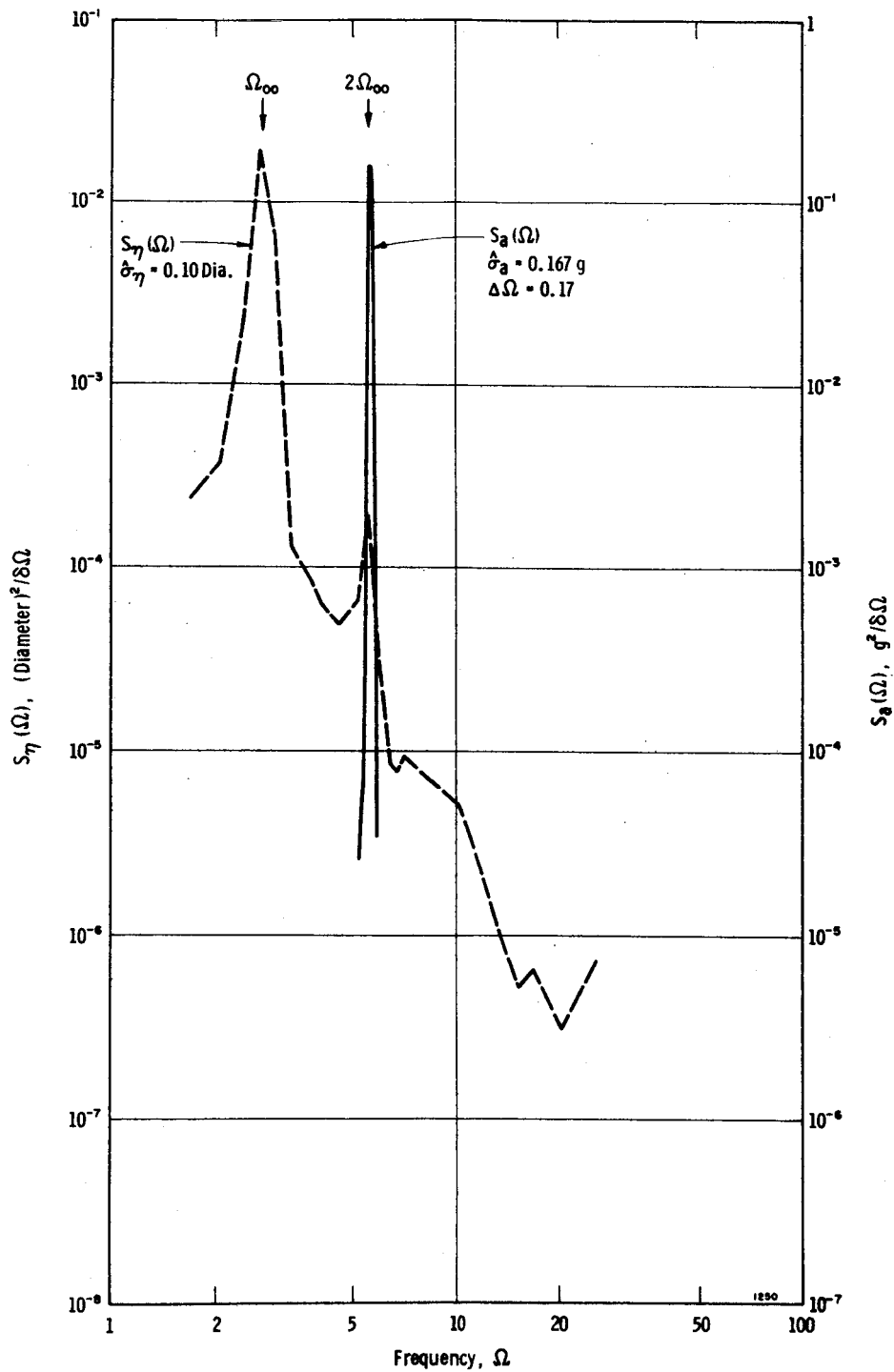
Figure 11.   Spectra: Very Narrow Band Random Excitation,
$\Delta\Omega = 0.17$, Maximum Excitation Level
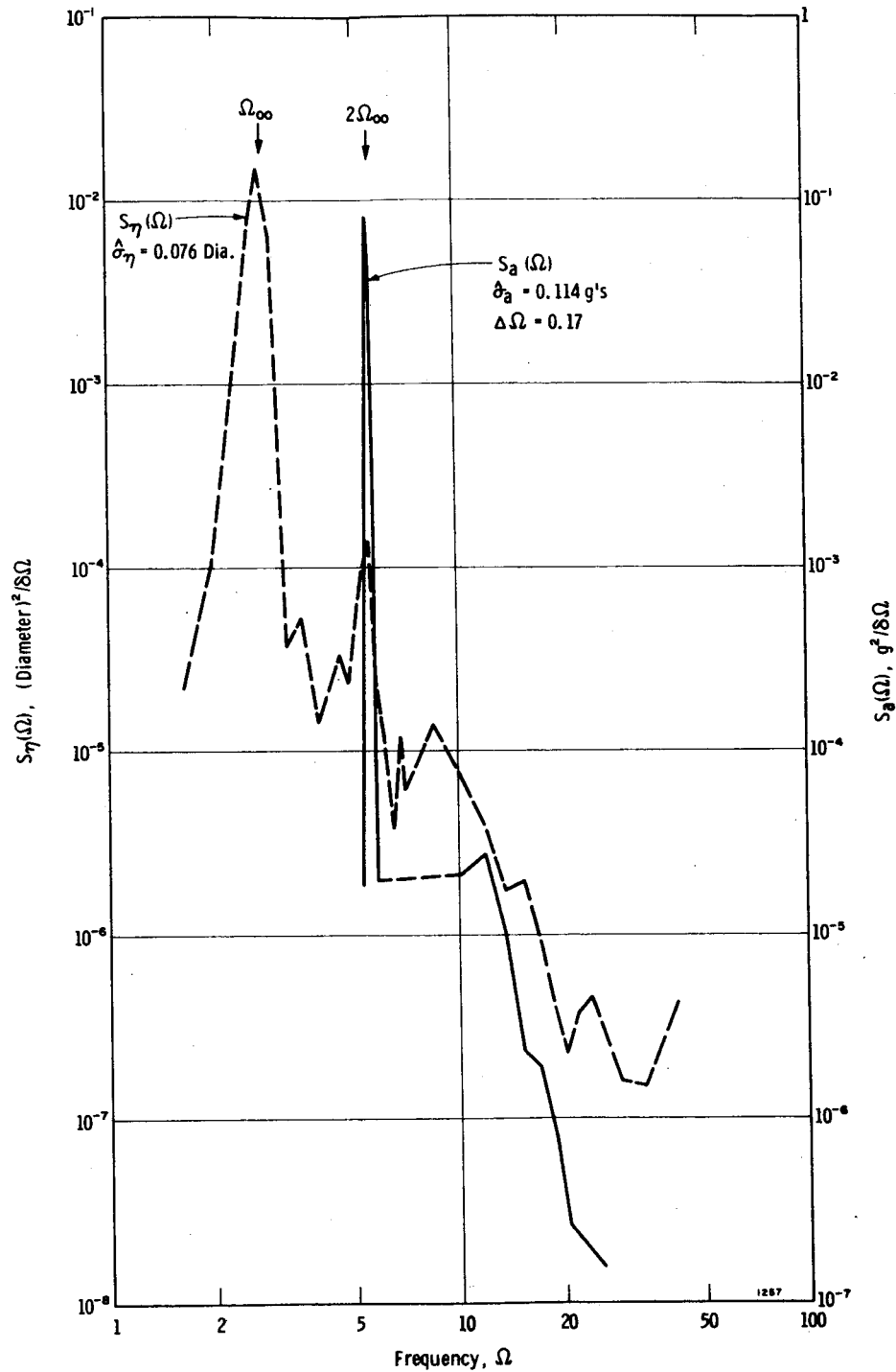
Figure 12.   Spectra: Very Narrow Band Random Excitation,
$\Delta\Omega = 0.17$, Medium Excitation Level
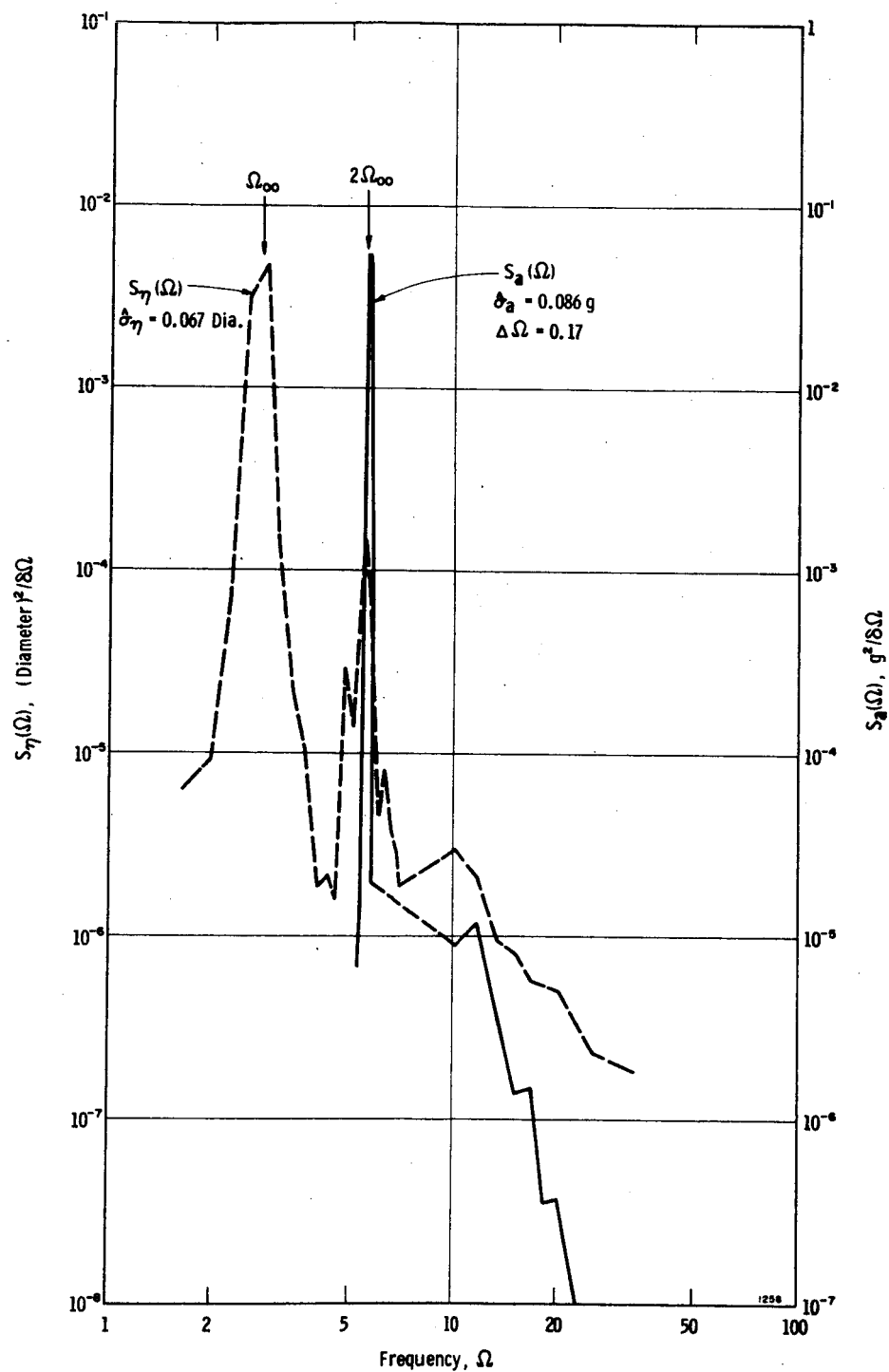
Figure 13. Spectra: Very Narrow Band Random Excitation,
$\Delta \Omega = 0.17$, Low Excitation Level
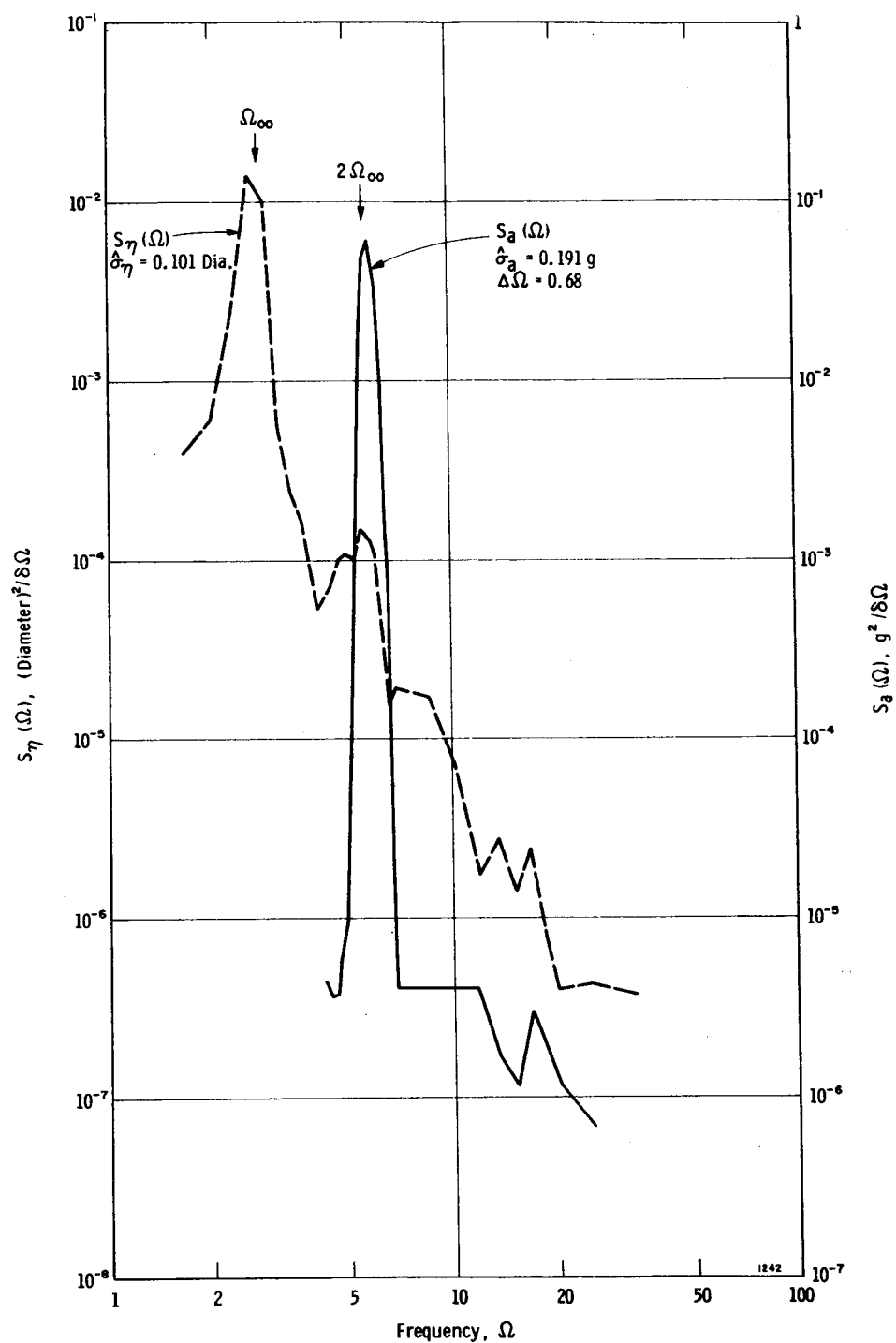
Figure 14.   Spectra: Very Narrow Band Excitation, $\Delta\Omega = 0.68$,
Maximum Excitation Level
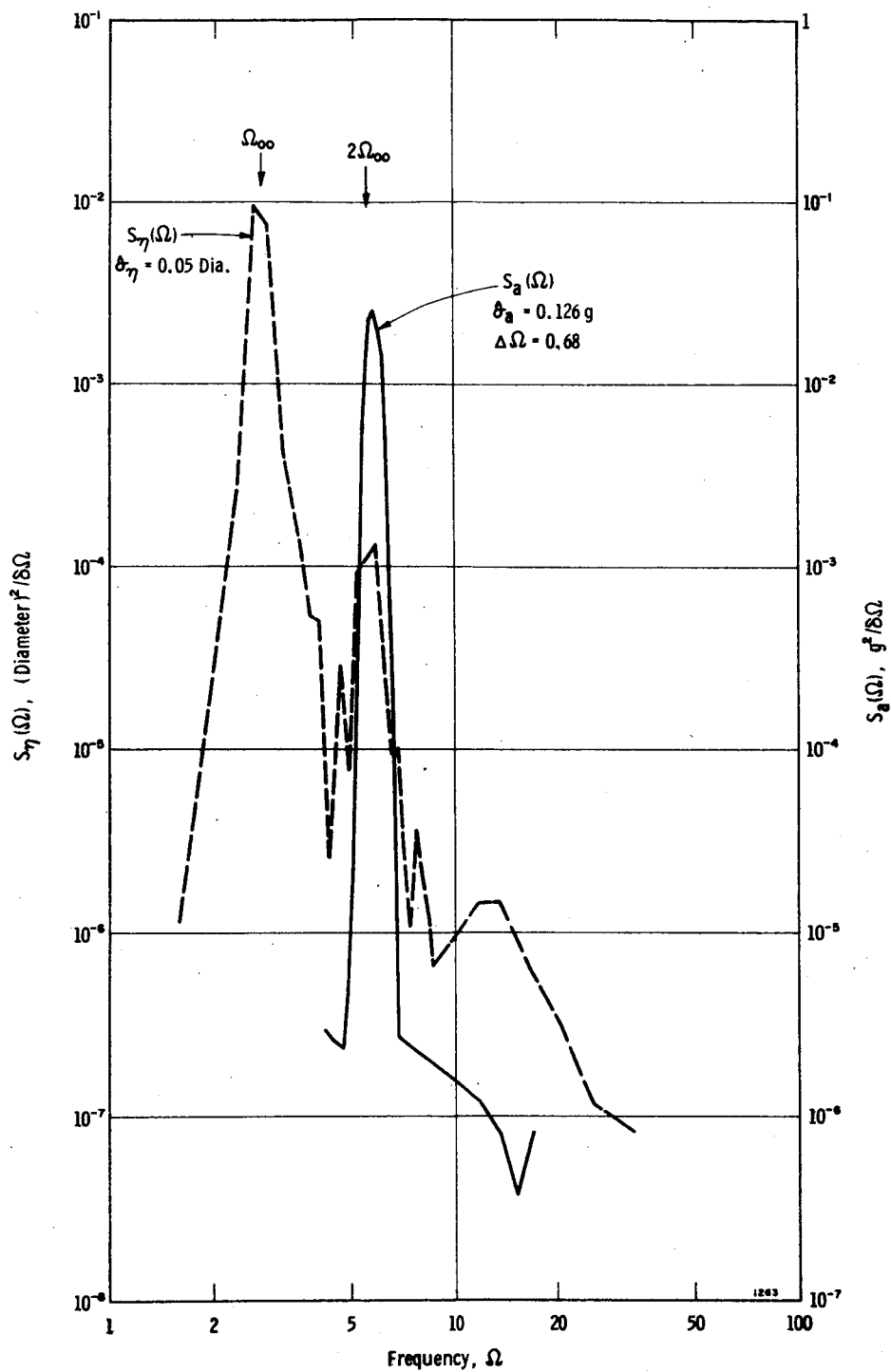
Figure 15. Spectra: Very Narrow Band Random Excitation,
$\Delta\Omega = 0.68$, Low Excitation Level
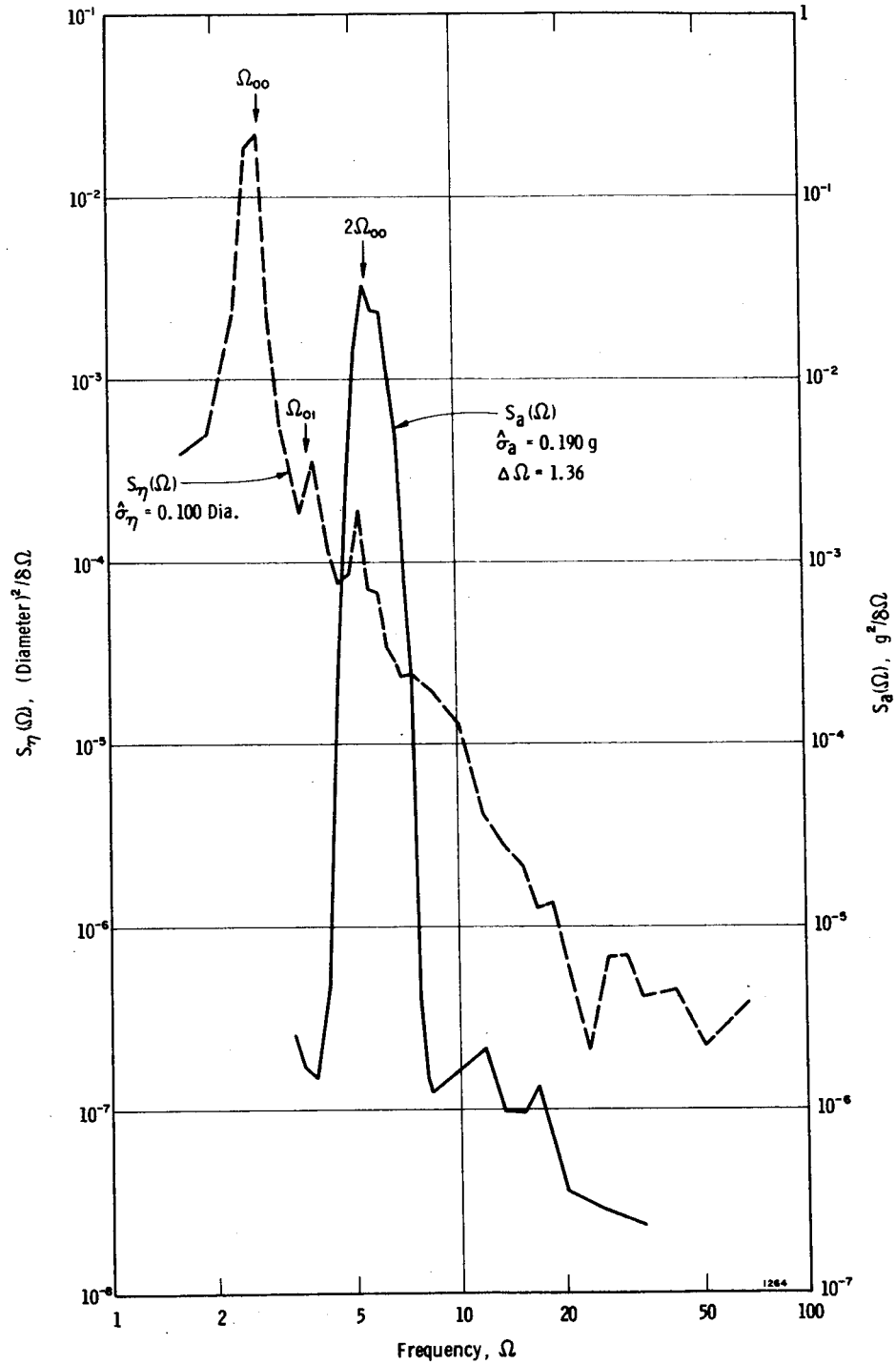
Figure 16. Spectra: Narrow Band Random Excitation,
$\Delta\Omega = 1.36$, Maximum Excitation Level

10^{-1} 1

10^{-2} 10^{-1}

$2\,\Omega_{\infty}$

10^{-3} 10^{-2}

$S_a(\Omega)$
$\hat{\sigma}_a = 0.124\,g$
$\Delta\Omega = 1.36$

$S_{\eta}(\Omega)$, (Diameter)^2/8Ω

10^{-4} 10^{-3}

$S_{\eta}(\Omega)$
$\hat{\sigma}_{\eta} = 0.0075$ Dia.

$S_a(\Omega)$, g^2/8Ω

10^{-5} 10^{-4}

Ω_{∞}

10^{-6} 10^{-5}

10^{-7} 10^{-6}

1265

10^{-8} 10^{-7}

1   2   5   10   20   50   100

Frequency, Ω
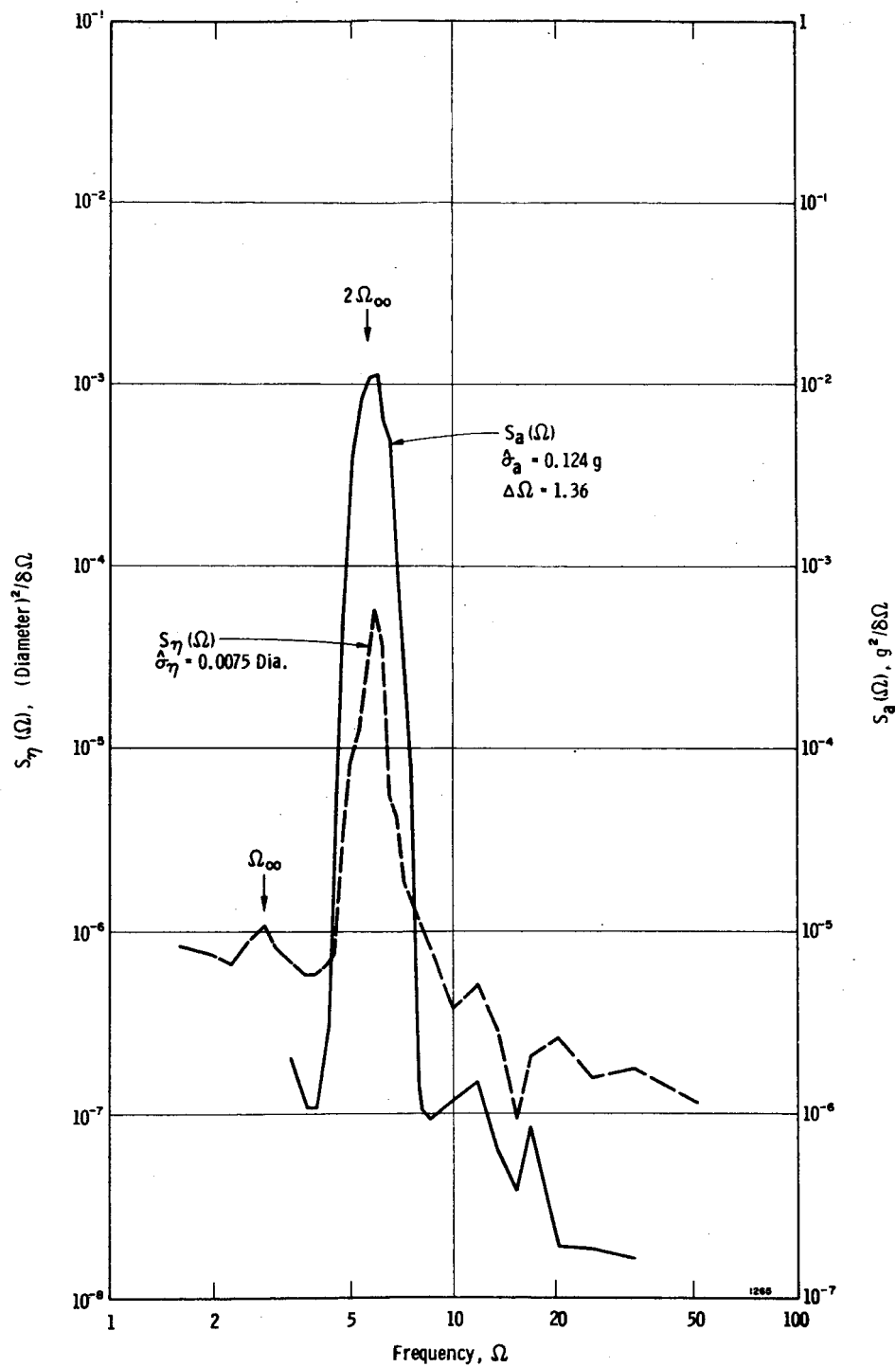
Figure 17. Spectra: Narrow Band Random Excitation,
$\Delta\Omega = 1.36$, Low Excitation Level
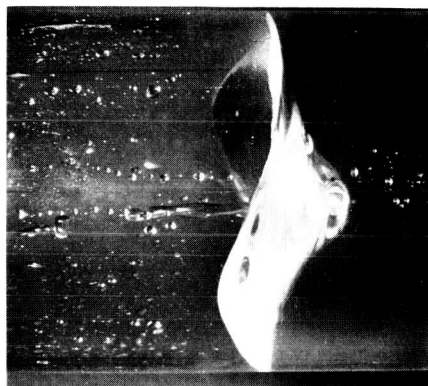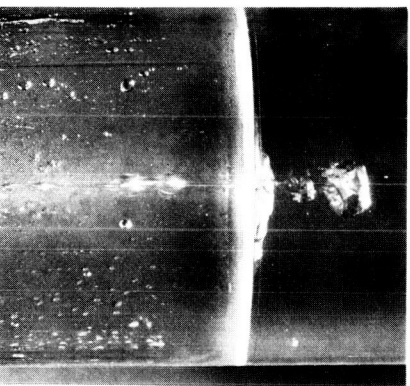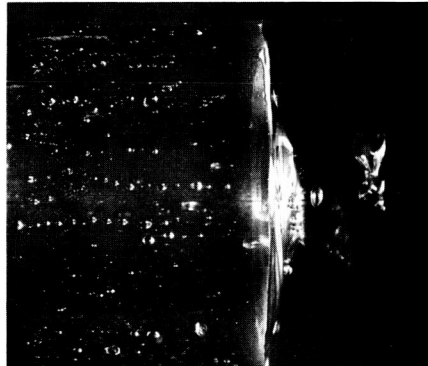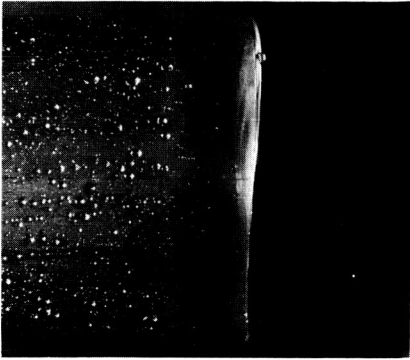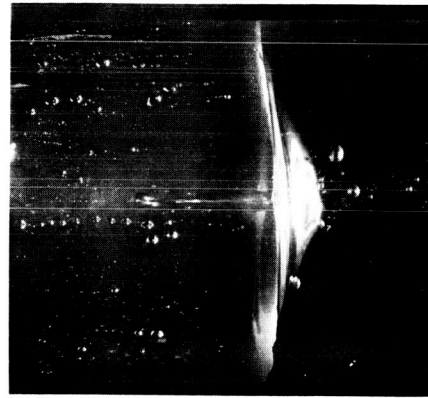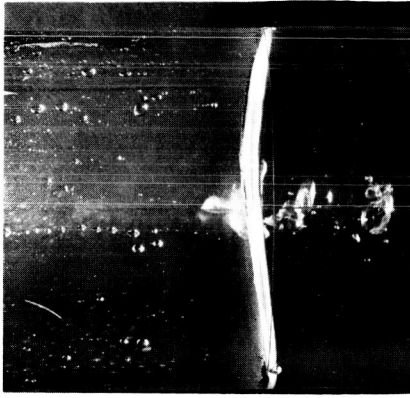
Figure 18. Stills Taken At Random Instants Of Free Surface
Under The Experimental Conditions Of Figure 16
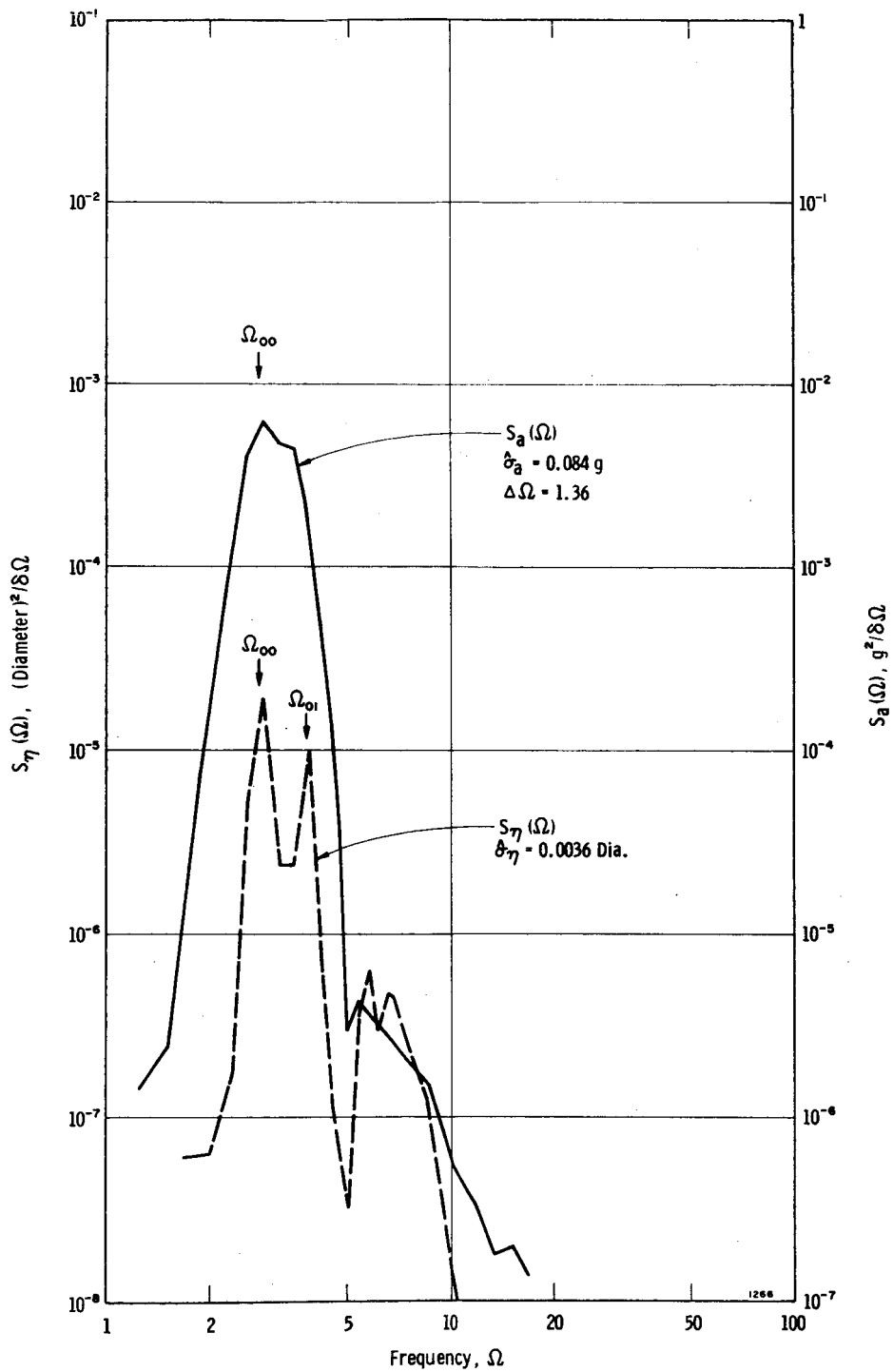
Figure 19. Spectra : Narrow Band Random Excitation Centered
On Frequency Of First Axi-Symmetric Mode
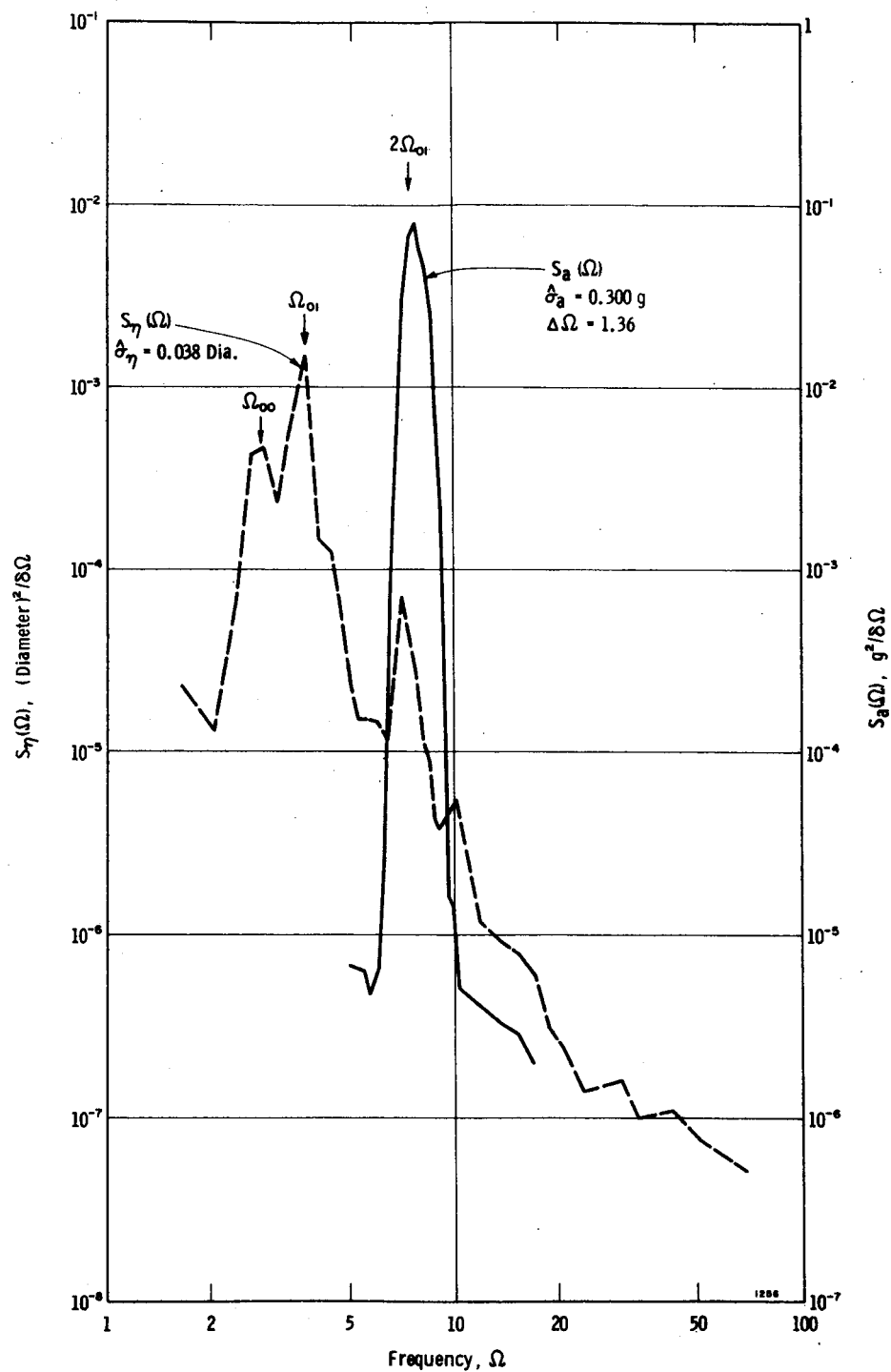
Figure 20.   Spectra: Narrow Band Random Excitation Centered On Twice
The Frequency Of The Second Axi-Symmetric Mode
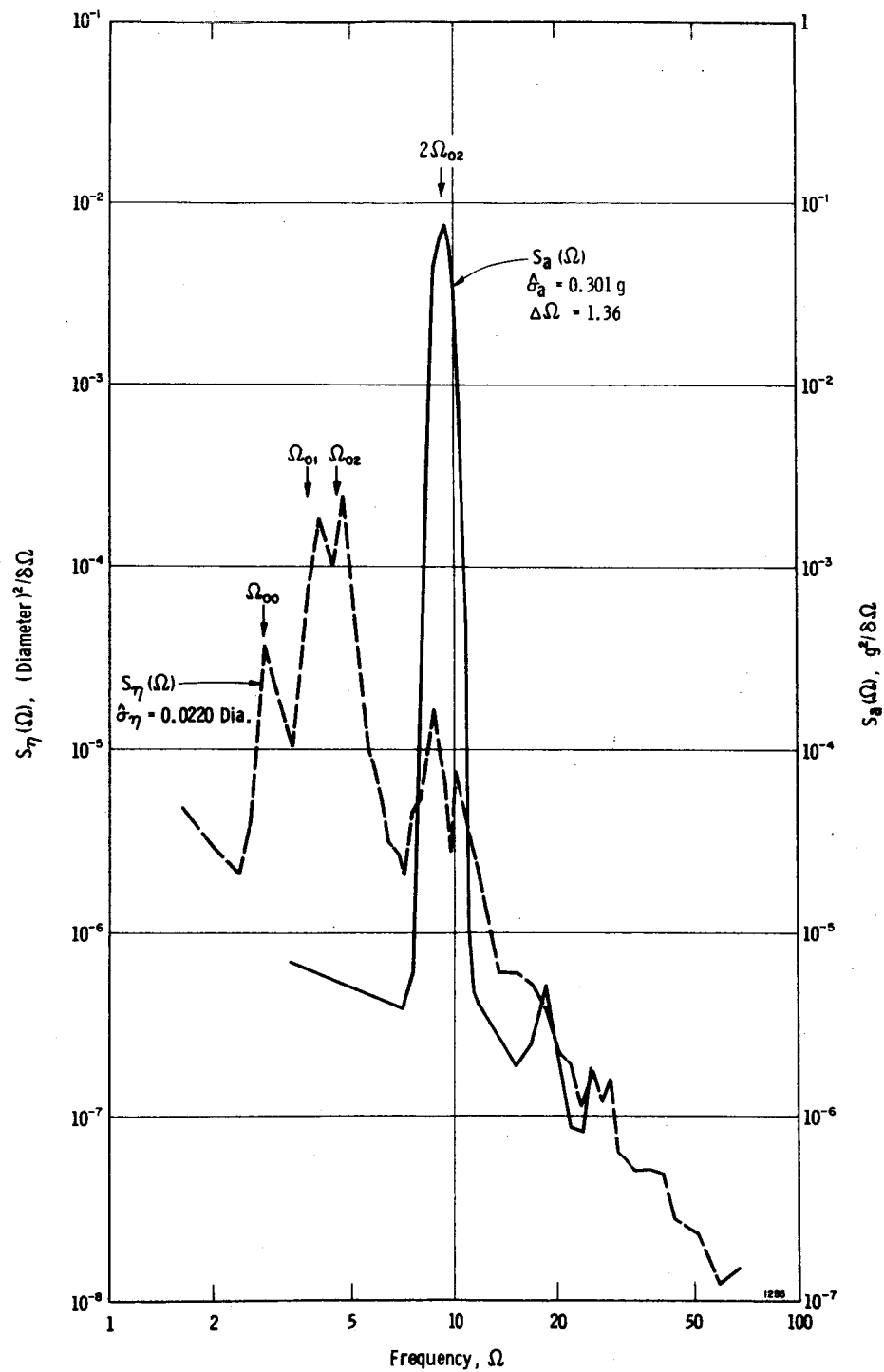
Figure 21. Spectra : Narrow Band Random Excitation Centered On Twice
The Frequency Of The Third Axi-Symmetric Mode
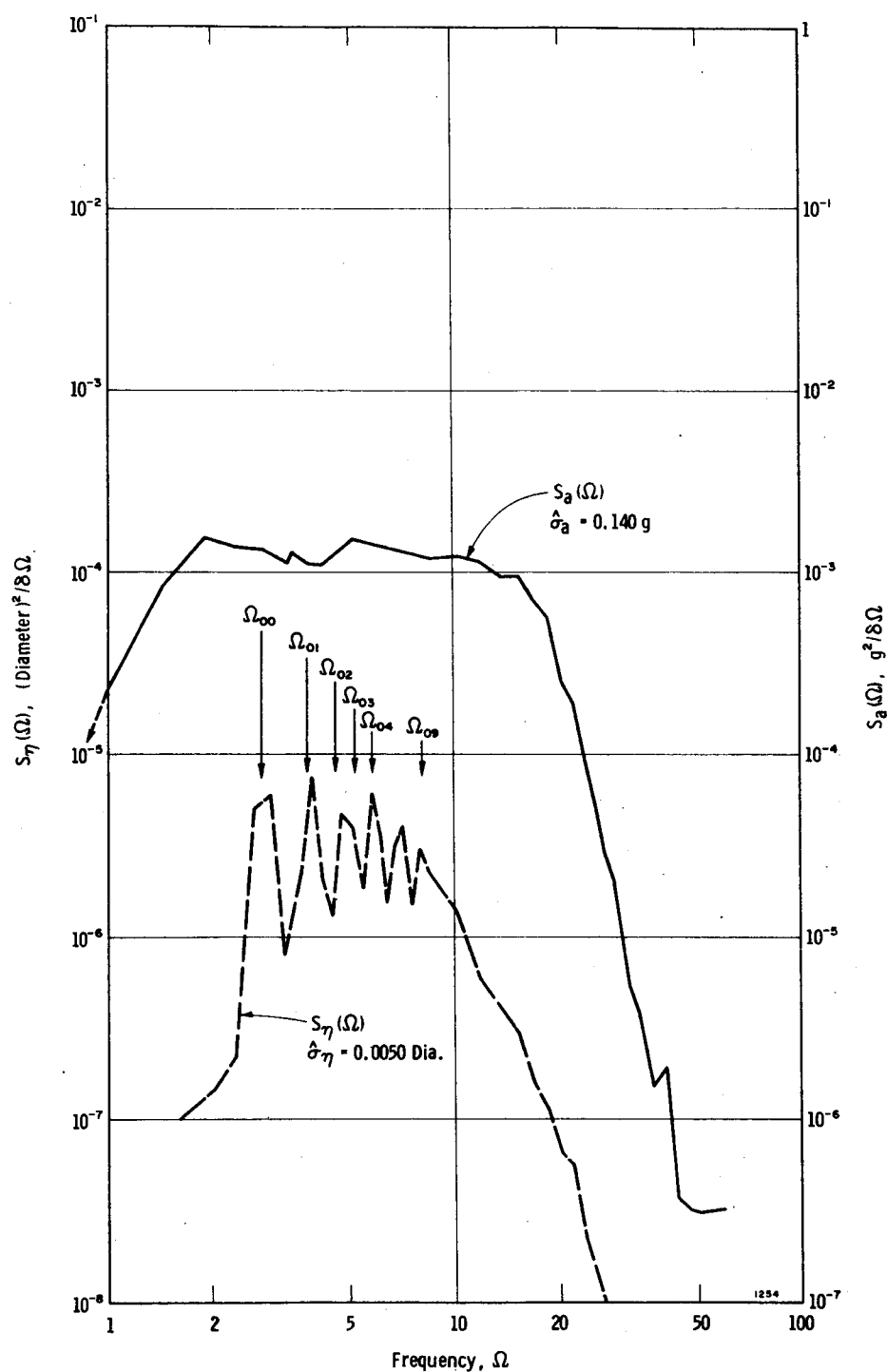
Figure 22. Spectra: Broad Band Random Excitation, Case 1
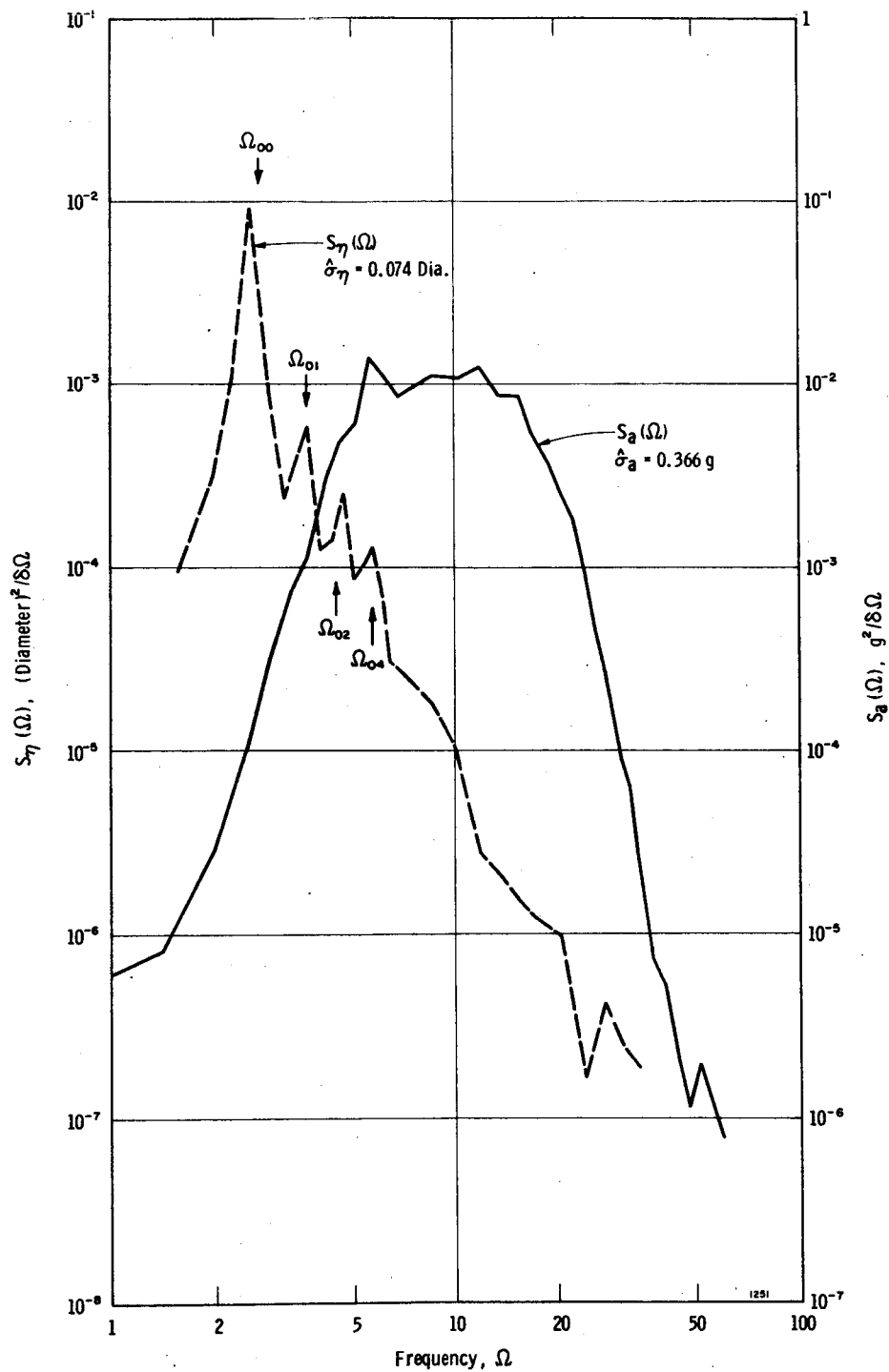
Figure 23. Spectra: Broad Band Random Excitation Case 2,
Maximum Excitation Level

10⁻¹

10⁻²

10⁻³

$S_\eta(\Omega)$, (Diameter)²/$\delta\Omega$

10^{-4}

$S_a(\Omega)$
$\hat{\vartheta}_a = 0.248\ g$

Ω_{02} Ω_{04}

Ω_{01}

10^{-5}

Ω_{00}

10^{-6}

$S_\eta(\Omega)$
$\hat{\vartheta}_\eta = 0.0103\ $Dia.

10^{-7}

10^{-8}

1   2   5   10   20   50   100

Frequency, Ω

$S_a(\Omega)$, g²/$\delta\Omega$

1

10⁻¹

10⁻²

10⁻³

10⁻⁴

10⁻⁵

10⁻⁶

10⁻⁷

1249
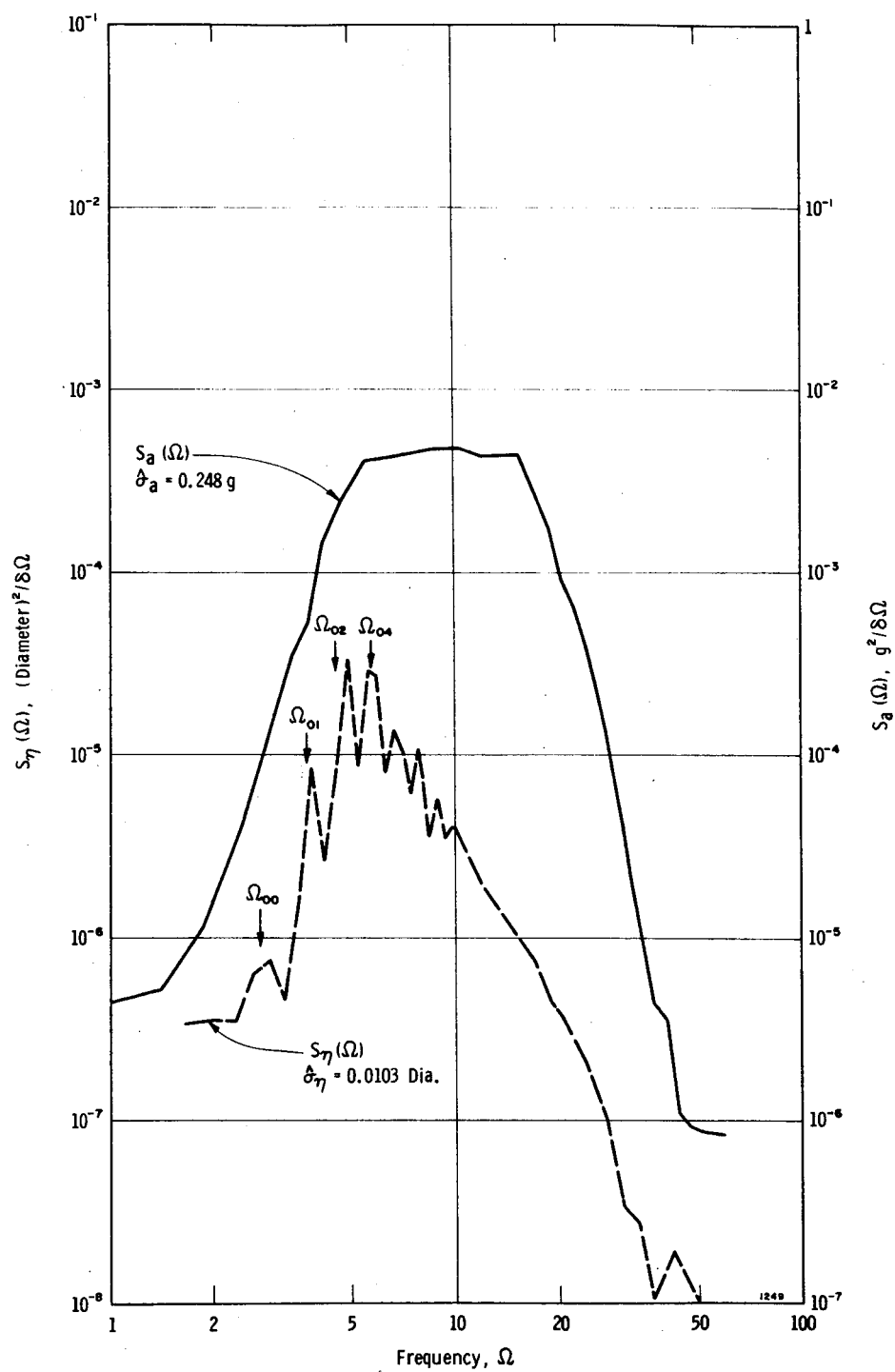
Figure 24. Spectra: Broad Band Random Excitation Case 2,
Low Excitation Level
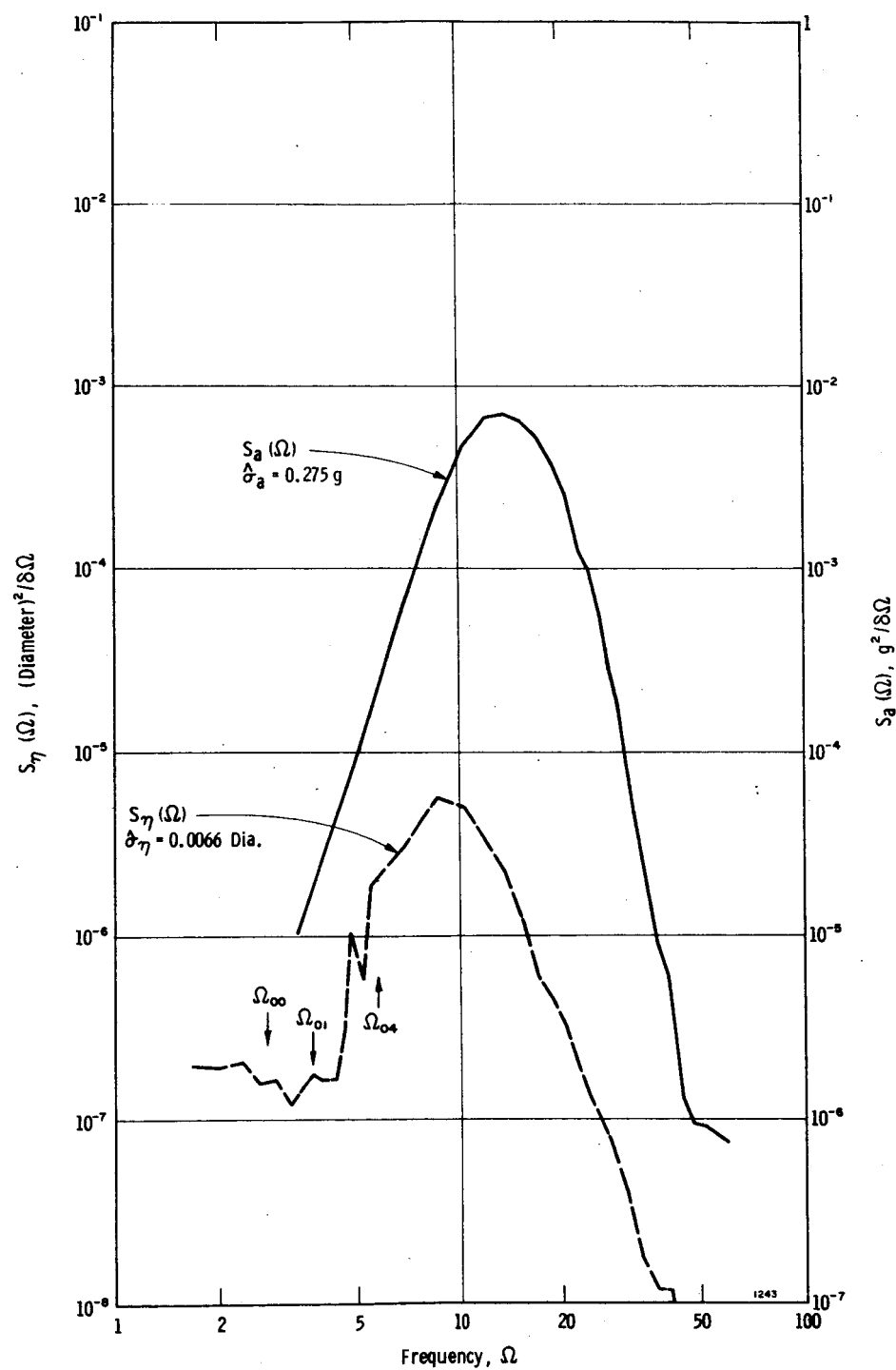
Figure 25. Spectra: Broad Band Random Excitation Case 3
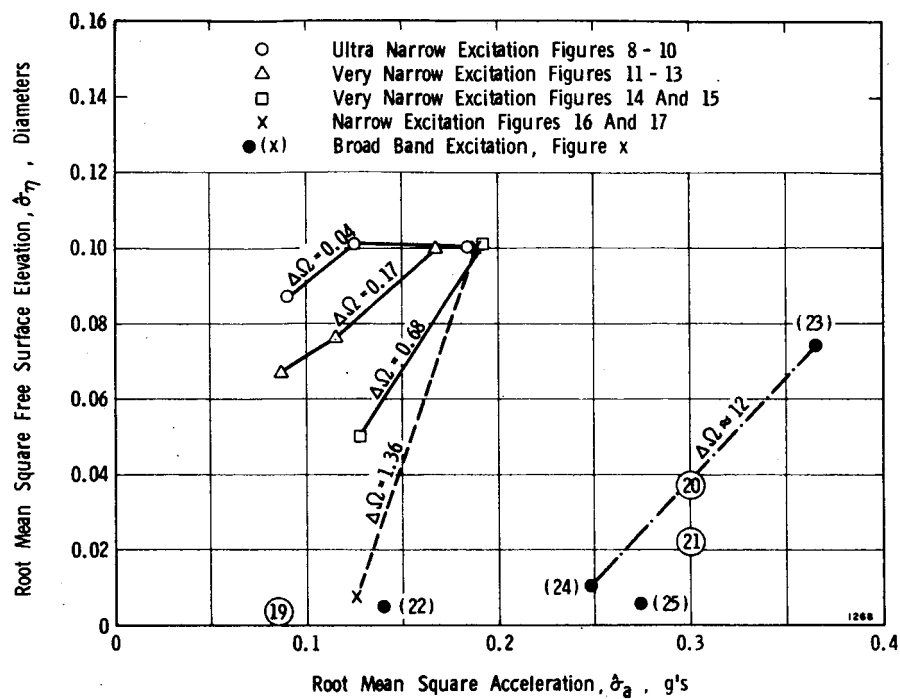
Figure 26. Summary Of rms Response For All Experiments

Acceleration Spectral Density Observed At
Twice The Frequency Of The Peak Surface
Elevation Spectral Density, $(g)^2/\delta\Omega$
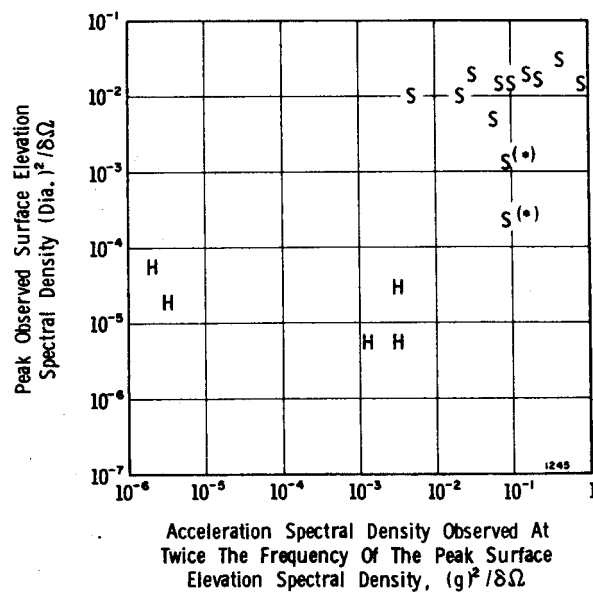
Figure 27. Correlations Of Spectral Densities
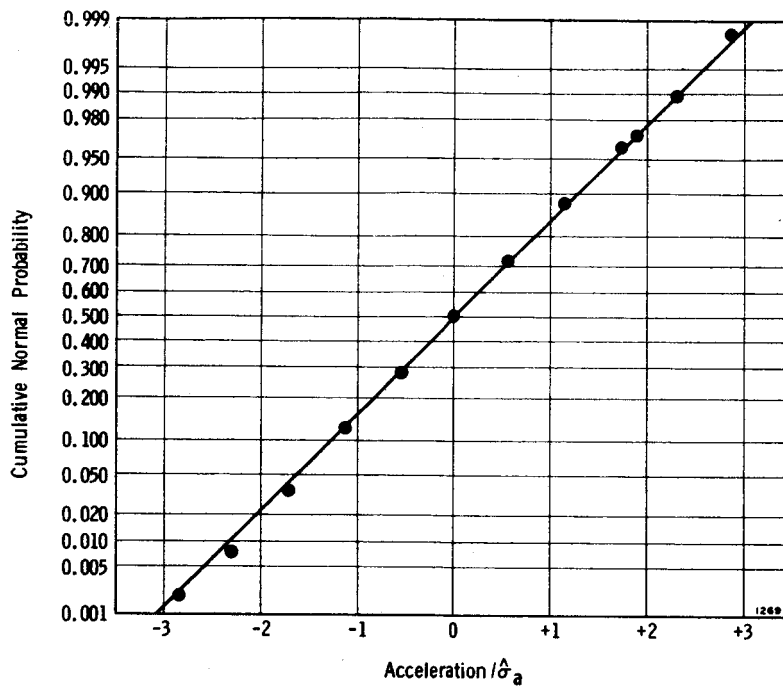
Figure 28. Typical Estimated Cumulative Probability - Acceleration, Narrow Band Excitation Corresponding To Figure 16
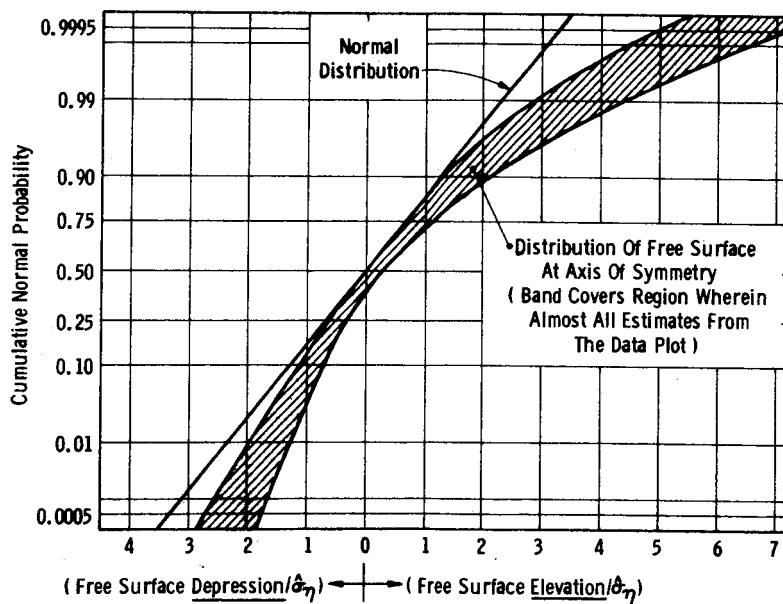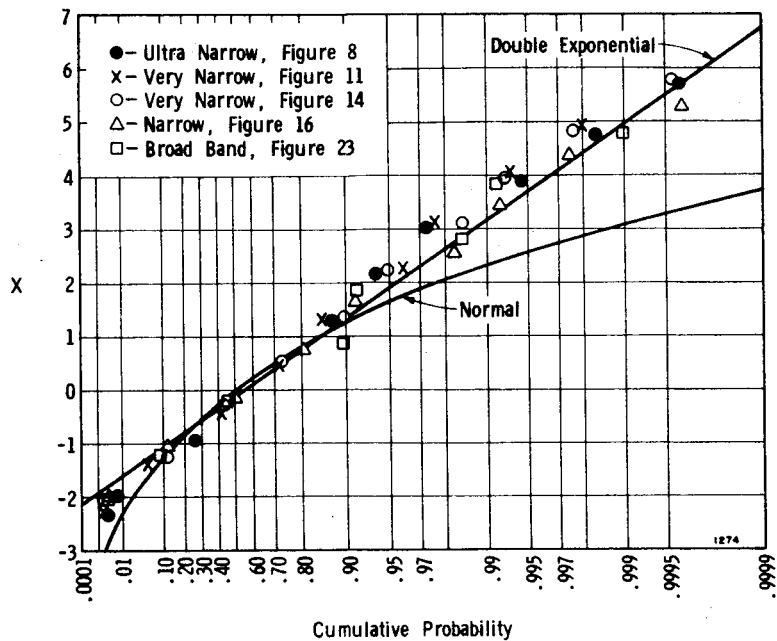

Figure 29. Distributions Of Free Surface Elevations, Normalized By The Sample Variance

Figure 30. Estimates Of Cumulative Probability Distribution Of Free
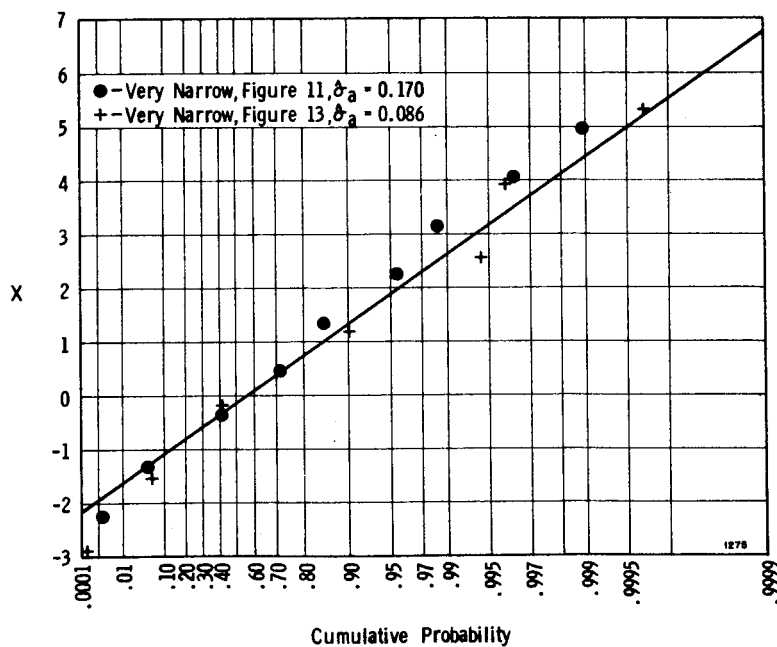Surface Elevations Plotted On Doubly Exponential
Probability Paper

Figure 31. Estimates Of Cumulative Probability Distribution Of Free
Surface Elevations. Plotted On Doubly Exponential
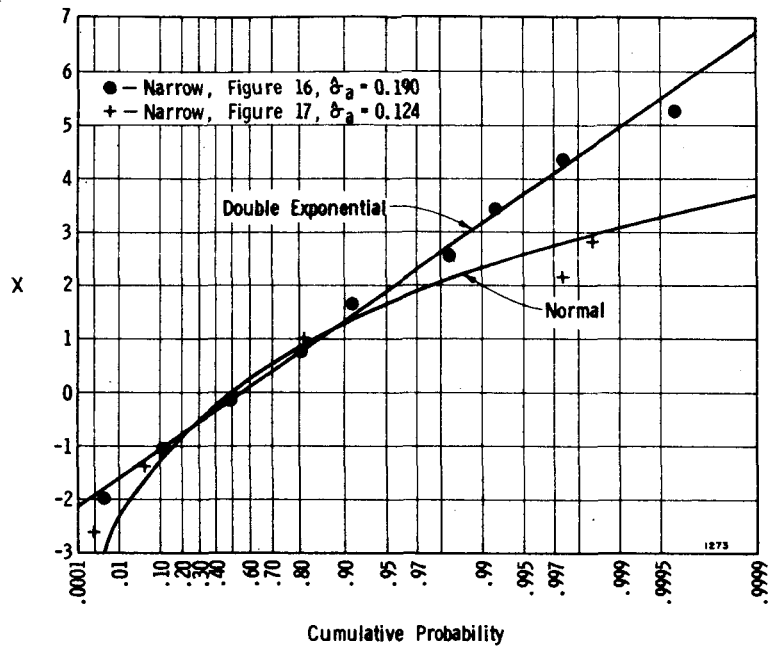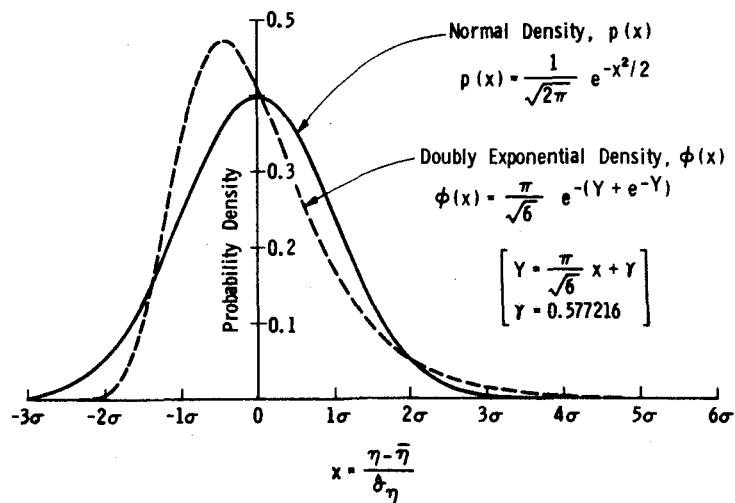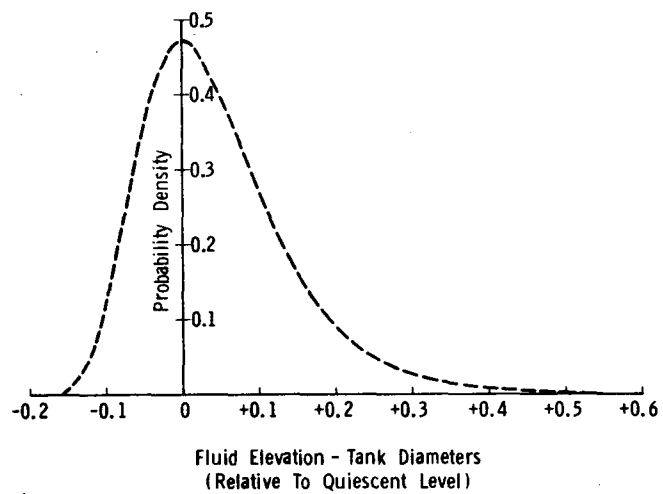Probability Paper

Figure 32. Estimates Of Cumulative Probability Distribution Of Free
Surface Elevations Plotted On Doubly Exponential
Probability Paper

Figure 33. Comparison Of Normal And Doubly
Exponential Probability Densities

Fluid Elevation - Tank Diameters
(Relative To Quiescent Level)

1244

Figure 34. Possible Probability Density For "1/2 Sub Harmonic"
Fluid Elevation On The Tank Axis
(Parameters Correspond To "Ultra Narrow
Band Excitation, Figure 8)